Physics of the atmosphere

LECTURE 5
THE ATMOSPHERIC BOUNDARY LAYER

B. Legras, legras@lmd.ens.fr, http://www.lmd.ens.fr/legras

2023

References : R. Stull, Boundary Layer Meteorology

S. Emeis, Surface-based remote sensing of the boundary layer

The good and the bad wind

- Windmill and modern aero-generators

- Joplin tornado, Missouri, 2011, 150 dead

I Introduction
I.1 Thickness and layering of the ABL

THE ATMOPHERIC BOUNDARY LAYER

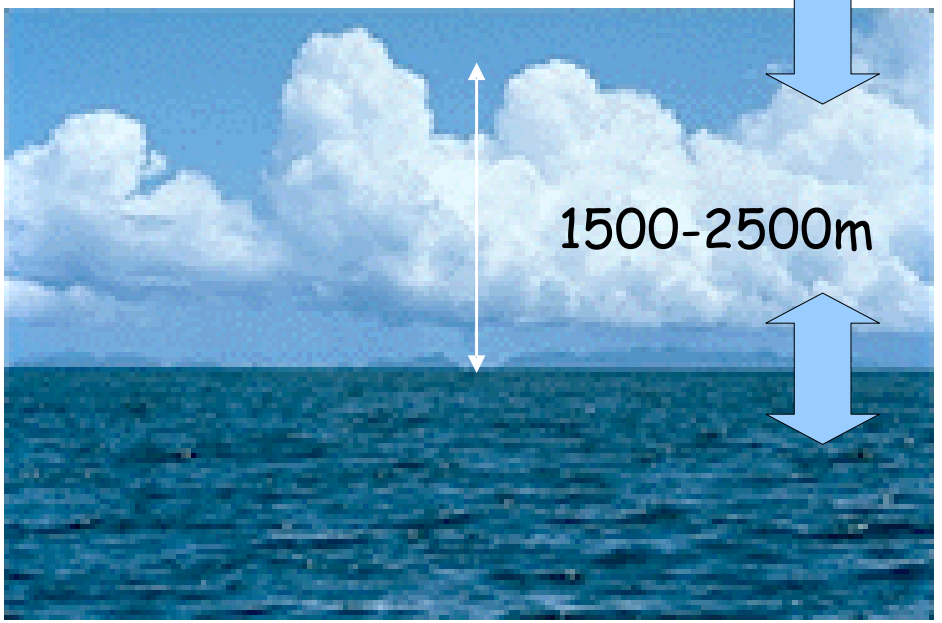

Exchanges with the free atmosphere

Ocean-atmosphere exchanges

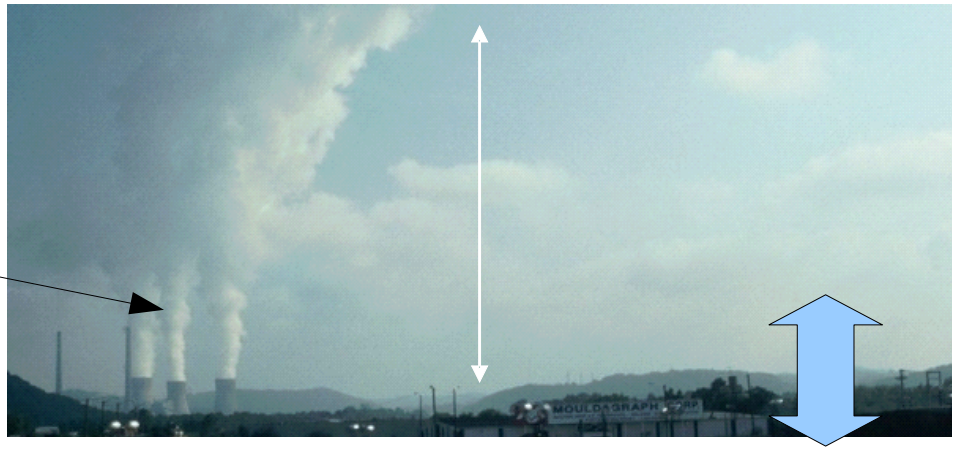

Emissions

Surface-atmosphere interactions

THE STRATIFIED STRUCTURE OF THE ABL

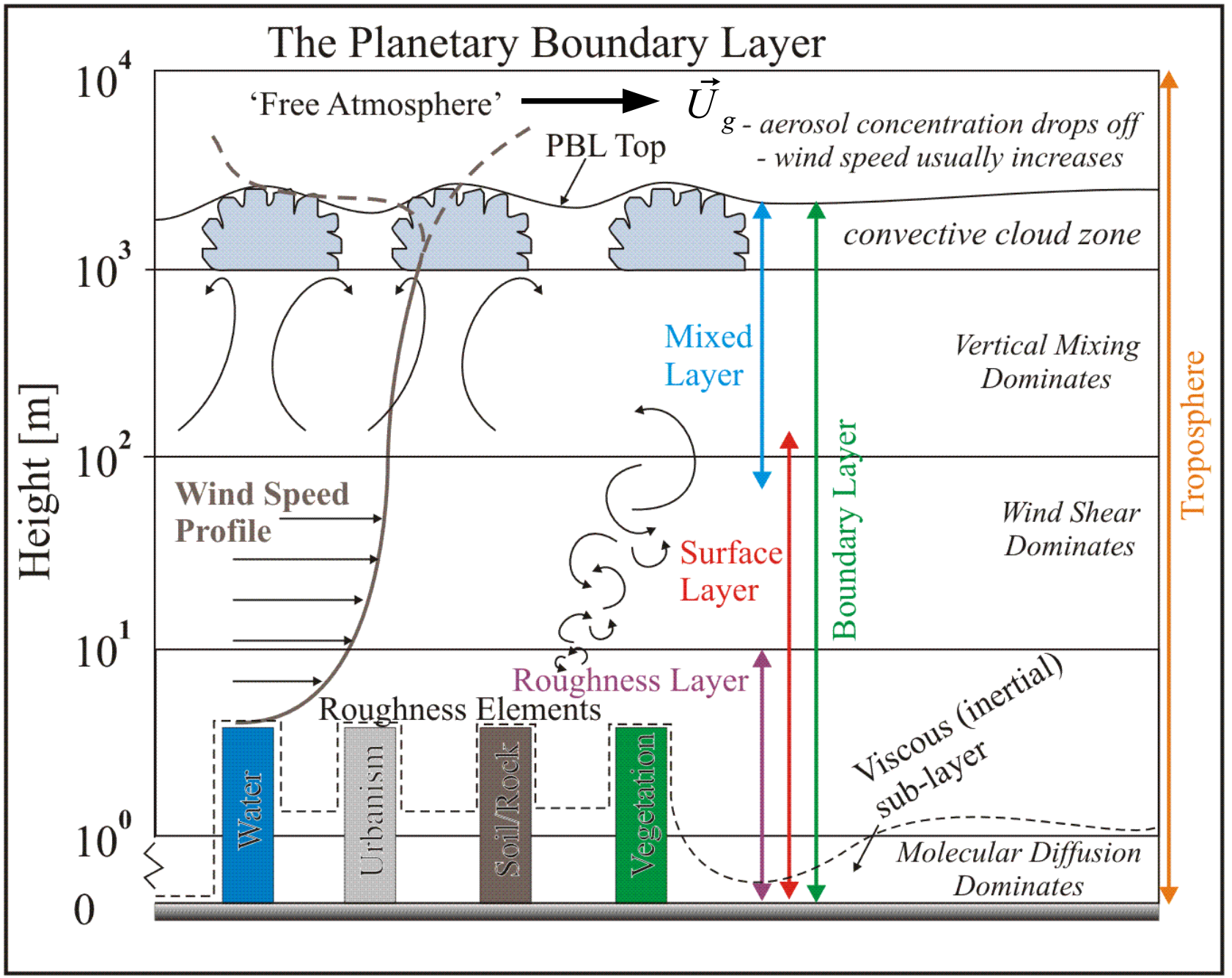

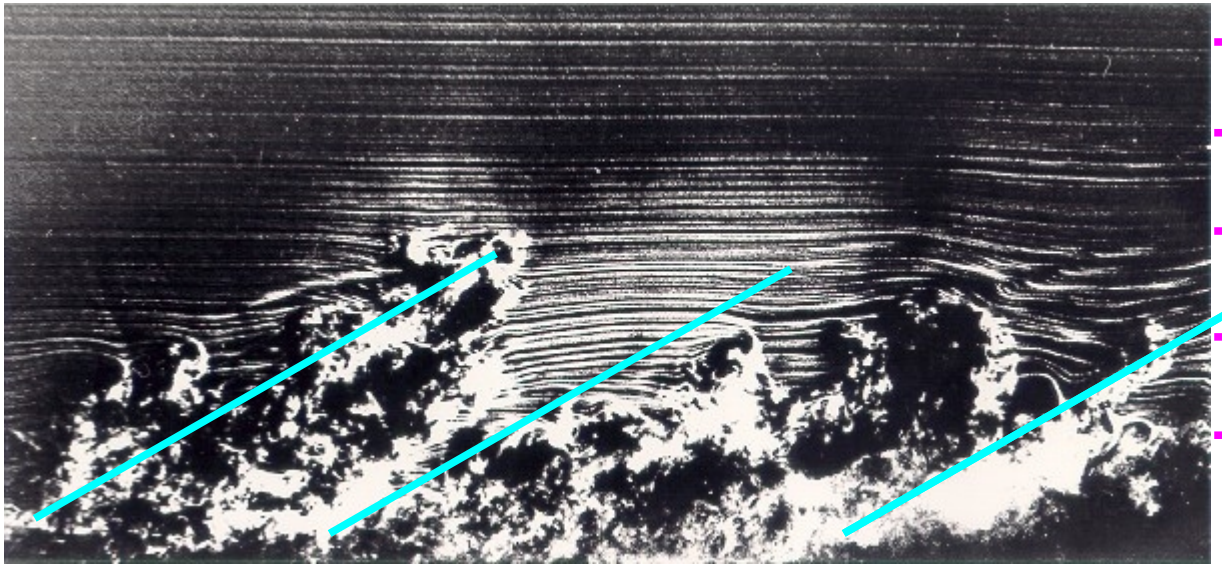

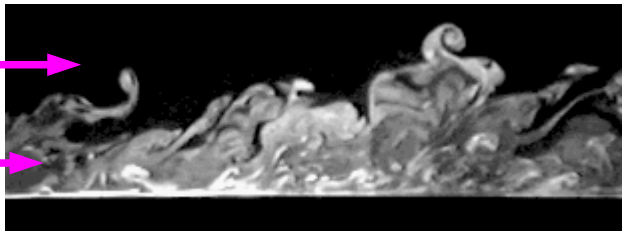

Speed

I. 2 SURFACE TURBULENT BOUNDARY LAYER

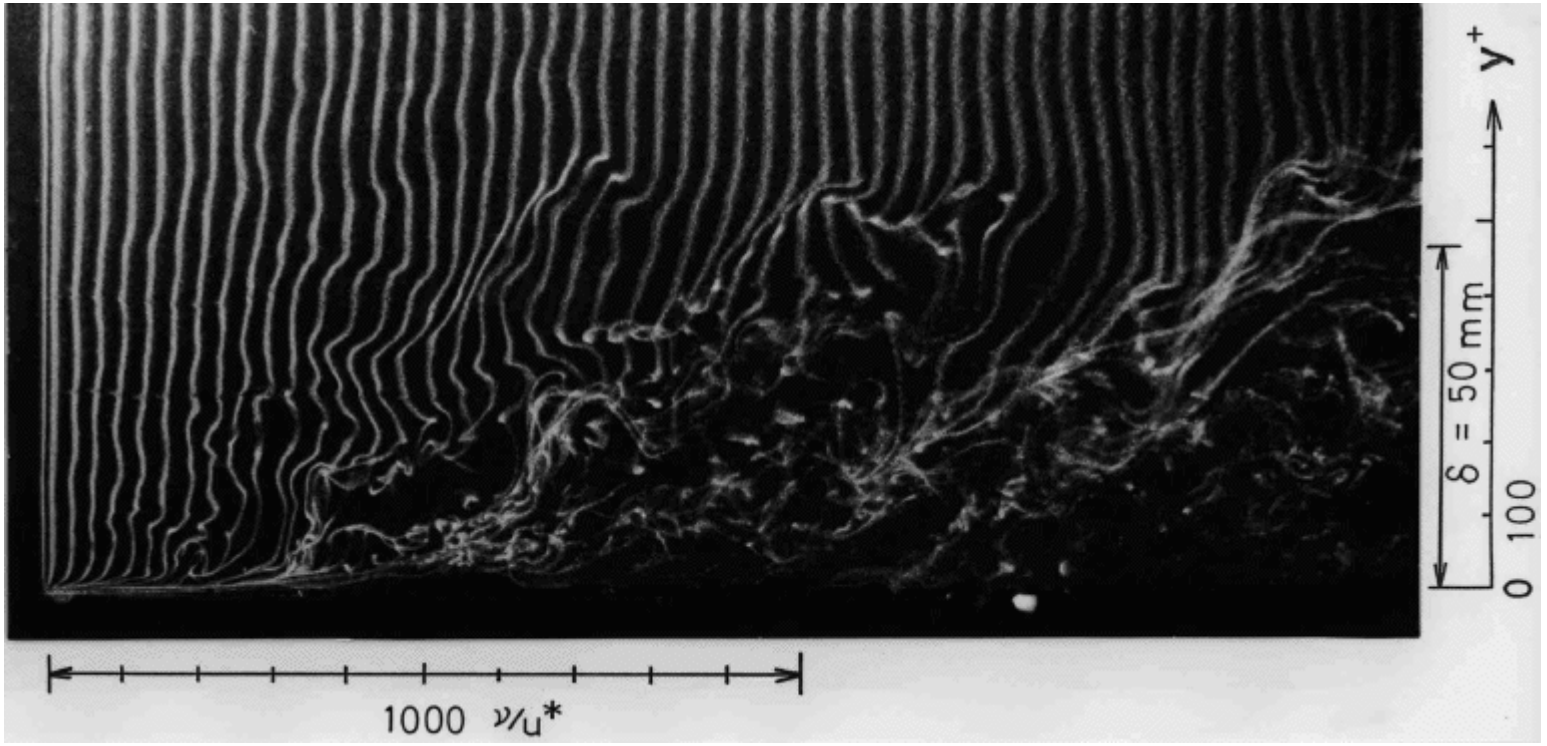

Rayleigh-Bénard convection

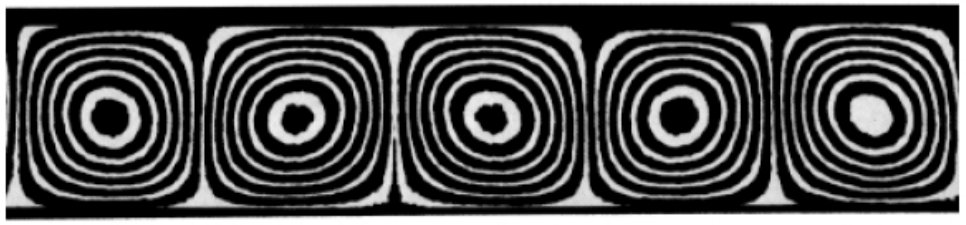

Slightly unstable convection in silicone oil van Dyke p. 82

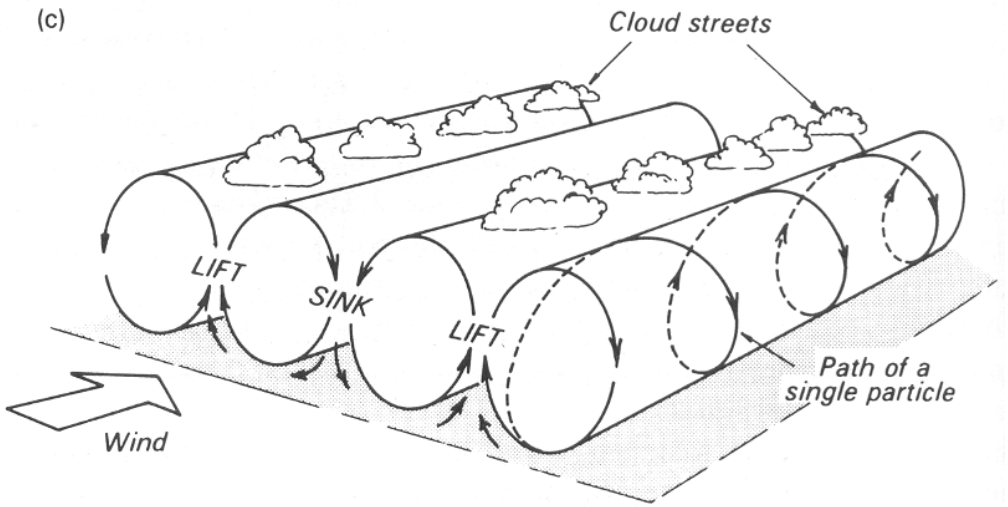

Figure 2.19 Convective structures associated with instability. (a) Stages in the temporal development of a thermal. (b) Initiation of a thermal by a hill. (c) Formation of cloud streets (based on Scorer, 1978).

Cloud street
Favorables for long distance glider flights.

Thermal stirring

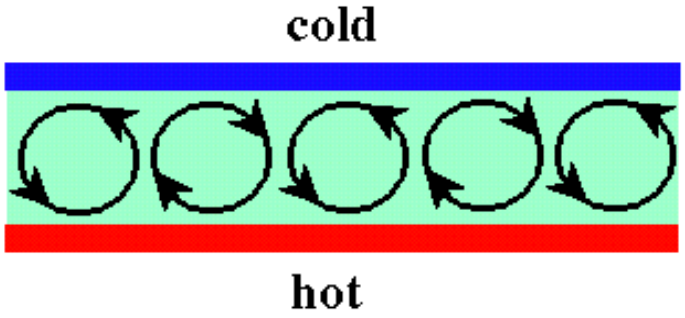

A fluid heated from its bottom boundary develops internal stirring motion that eventually mix the interior and makes temperature uniform but in two sharp boundary layers.

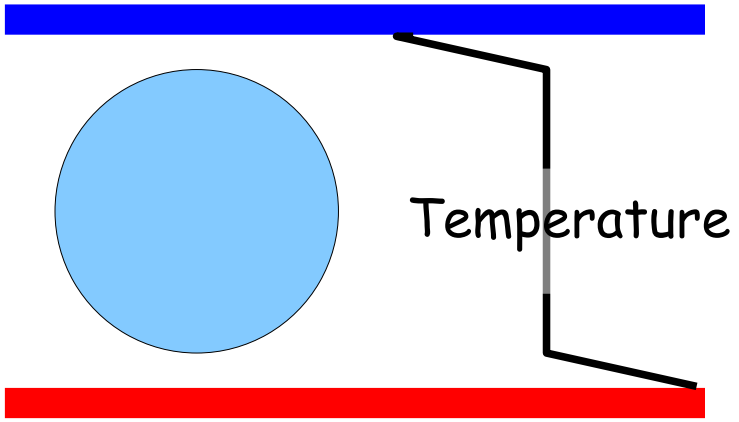

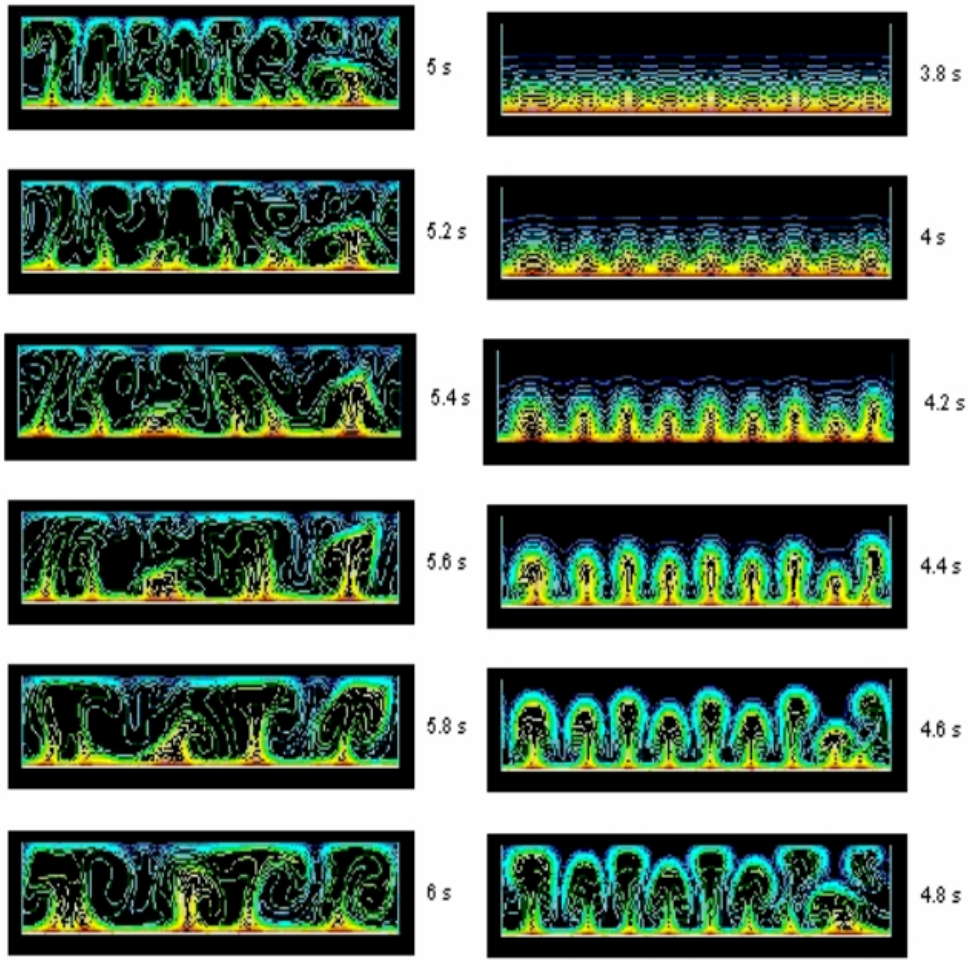

Thermal plumes in a fluid heated from below with a free surface. *Dinh et al., 2004*

I. 4 Thermal stirring in the stratified ABL

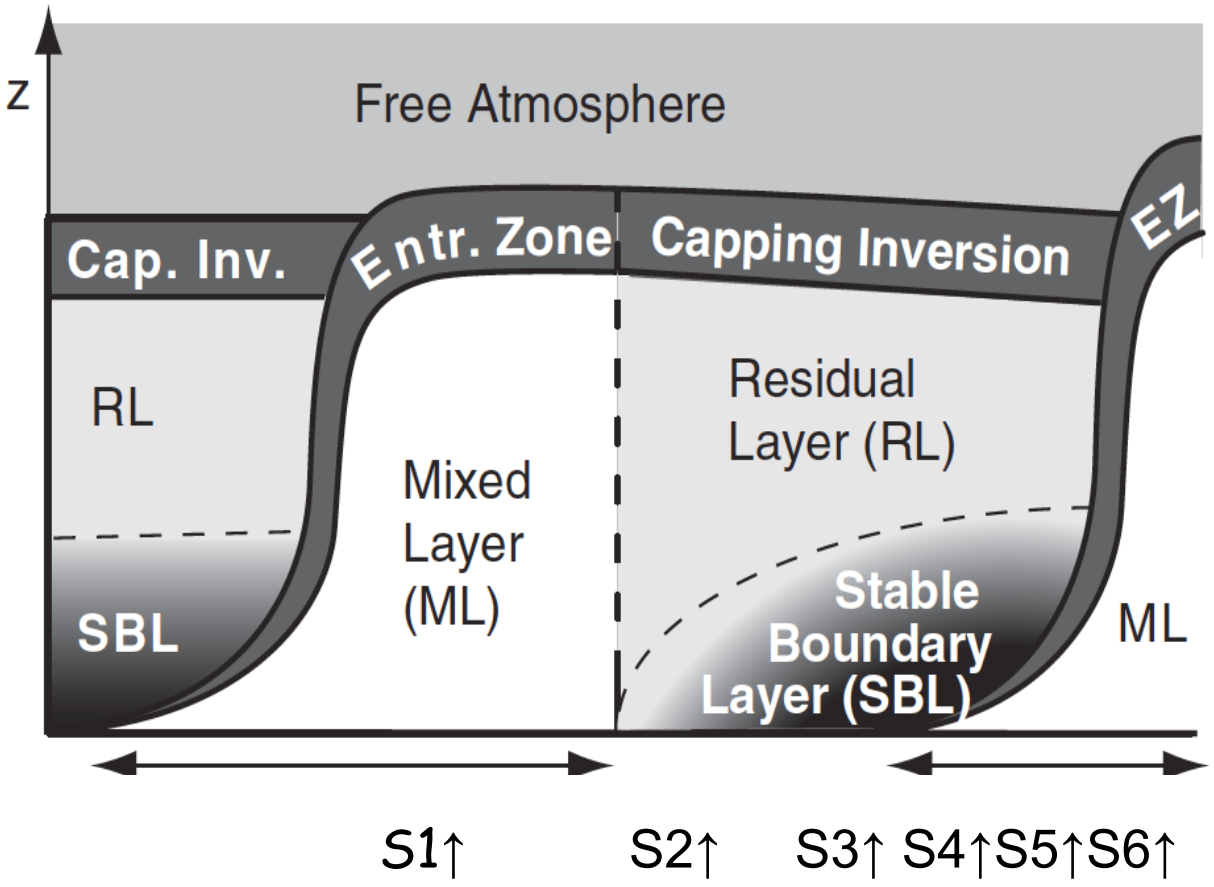

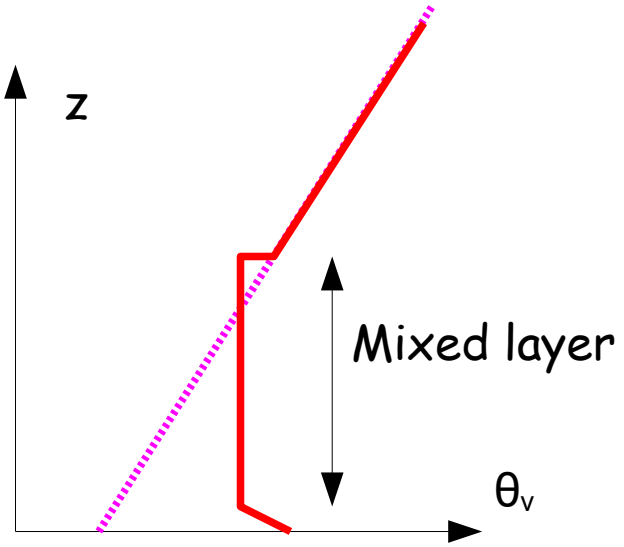

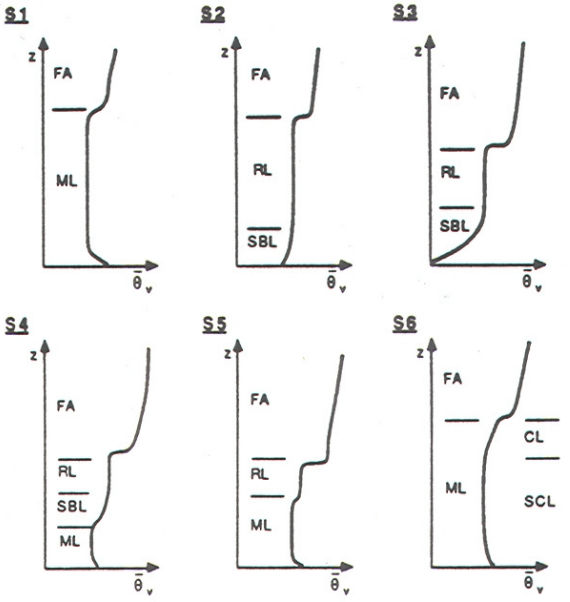

Diurnal cycle of the continental ABL under good weather. Mixing of the potential temperature $\theta_v=T_v(p0/p)^{R/Cp}$

Stull

Observation of the boundary layer aerosols + volcanic ashes by lidar (SIRTA)

Aérosol volcanique

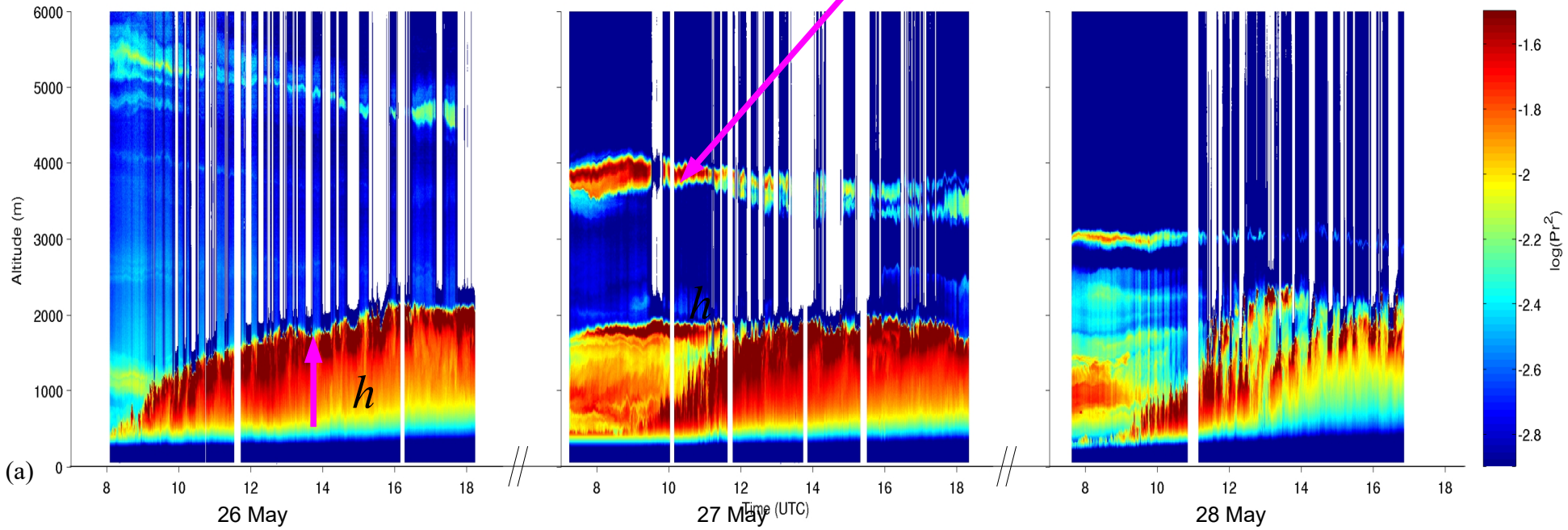

Diurnal cycle

$h \sim \sqrt{t}$

Lidar

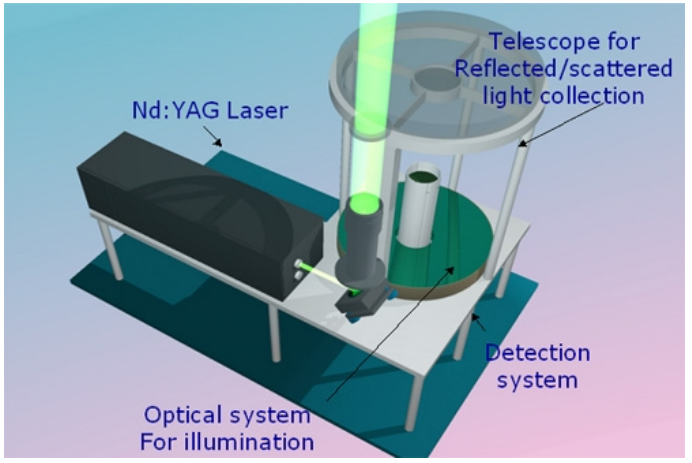

VON KARMAN VORTEX STREET

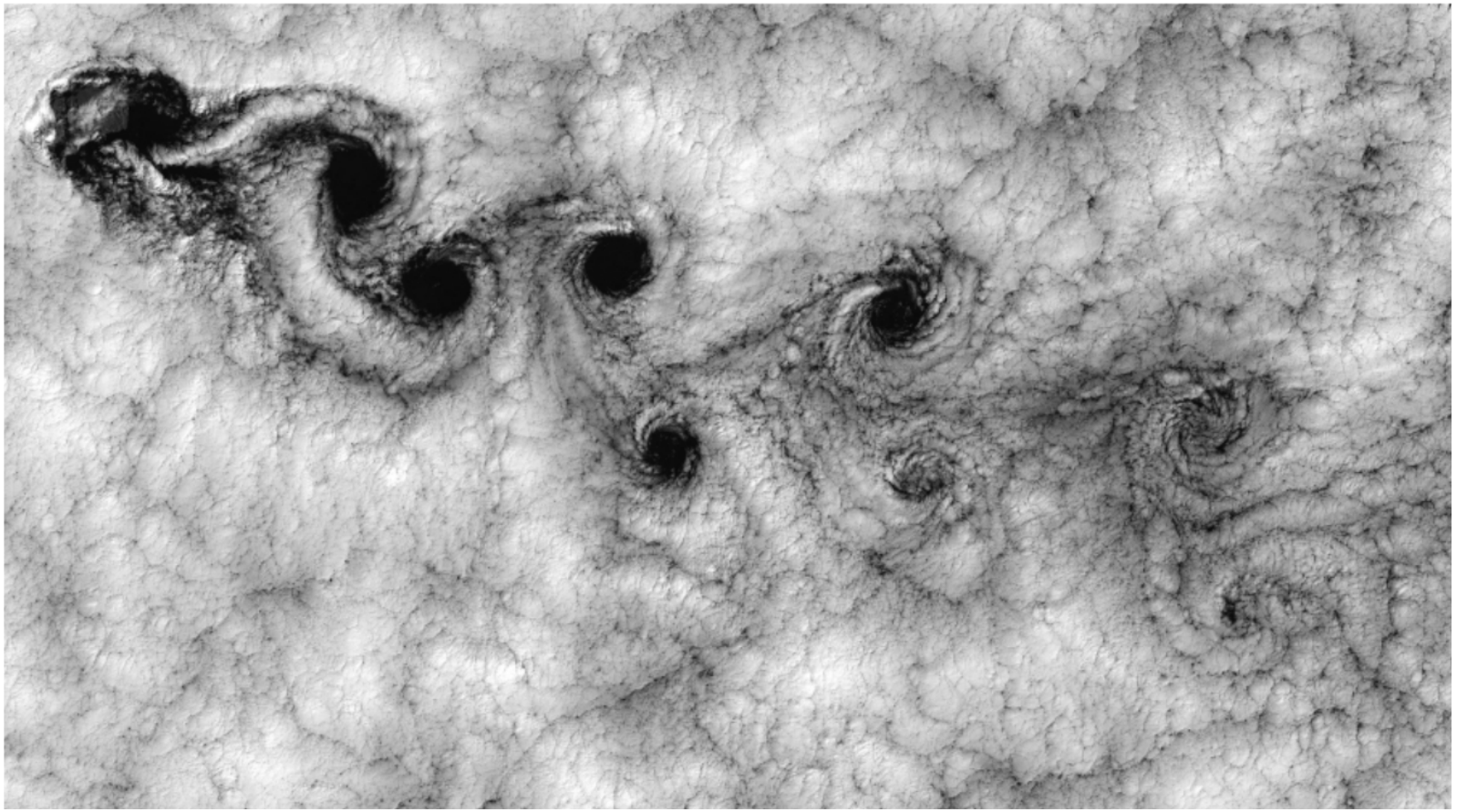

KELVIN-HELMHOLTZ INSTABILITY

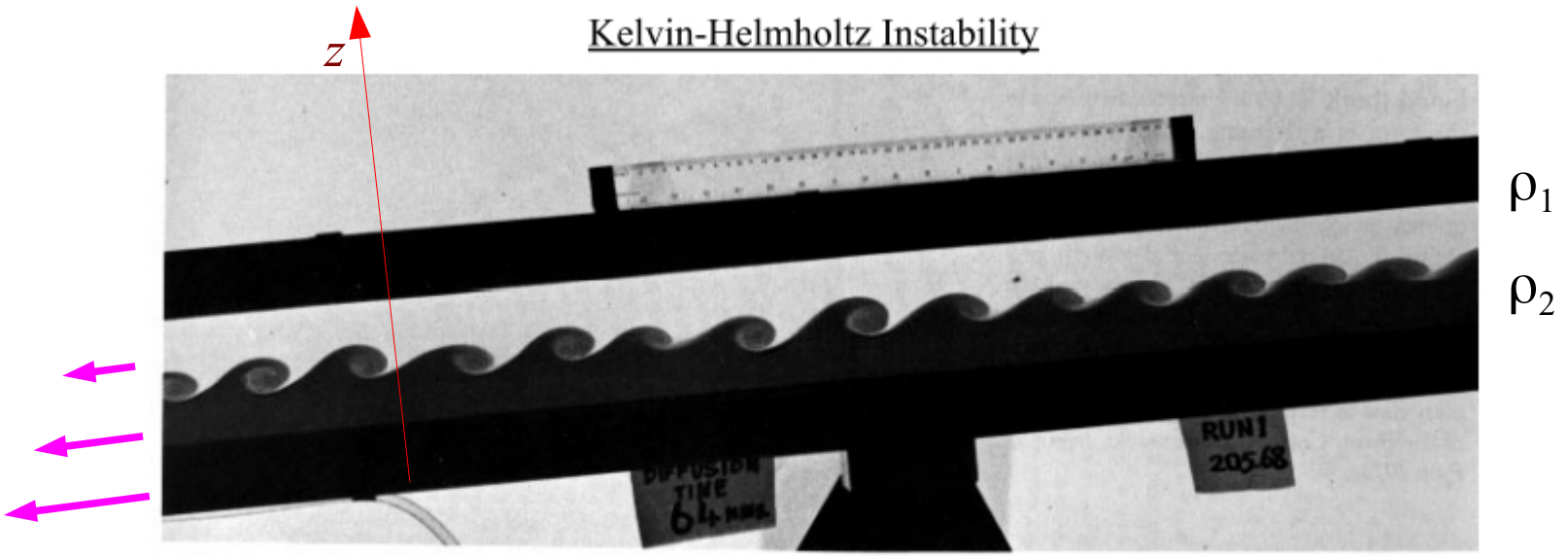

145. Kelvin-Helmholtz instability of stratified shear flow. A long rectangular tube, initially horizontal, is filled with water above colored brine. The fluids are allowed to diffuse for about an hour, and the tube then quickly tilted six degrees, setting the fluids into motion. The brine accelerates uniformly down the slope, while the water above similarly accelerates up the slope. Sinusoidal instability of the interface occurs after a few seconds, and has here grown nonlinearly into regular spiral rolls. *Thorpe 1971*

van Dyke, p. 85

Stratified fluid $\rho_2 > \rho_1$

Shear $\frac{dU}{dz}$

Brünt-Vaissala frequency $N^2 = \frac{g}{\rho}\frac{d\rho}{dz}$

Richardson number $Ri = \frac{N^2}{\left(\frac{dU}{dz}\right)^2}$

$Ri < 0{,}25$ somewhere is a necessary condition for instability

$Ri > 0{,}25$ everywhere is a sufficient condition for stability

KELVIN-HELMHOLTZ INSTABILITY

CLOUD ROLLS

Morning Glory, Carpentaria Gulf

FOEHN EFFECT

Lord Howe island

Pile of lenticular clouds above the Fujiyama

FAKE NEWS : The true image ! Beware of photoshop transformations that generate a number of spectacular images of natural phenomena found on the web.

Monbacho volcanoe

Other exemples of lenticular clouds (not fake).

I. 6 DOWNWARD FLUX

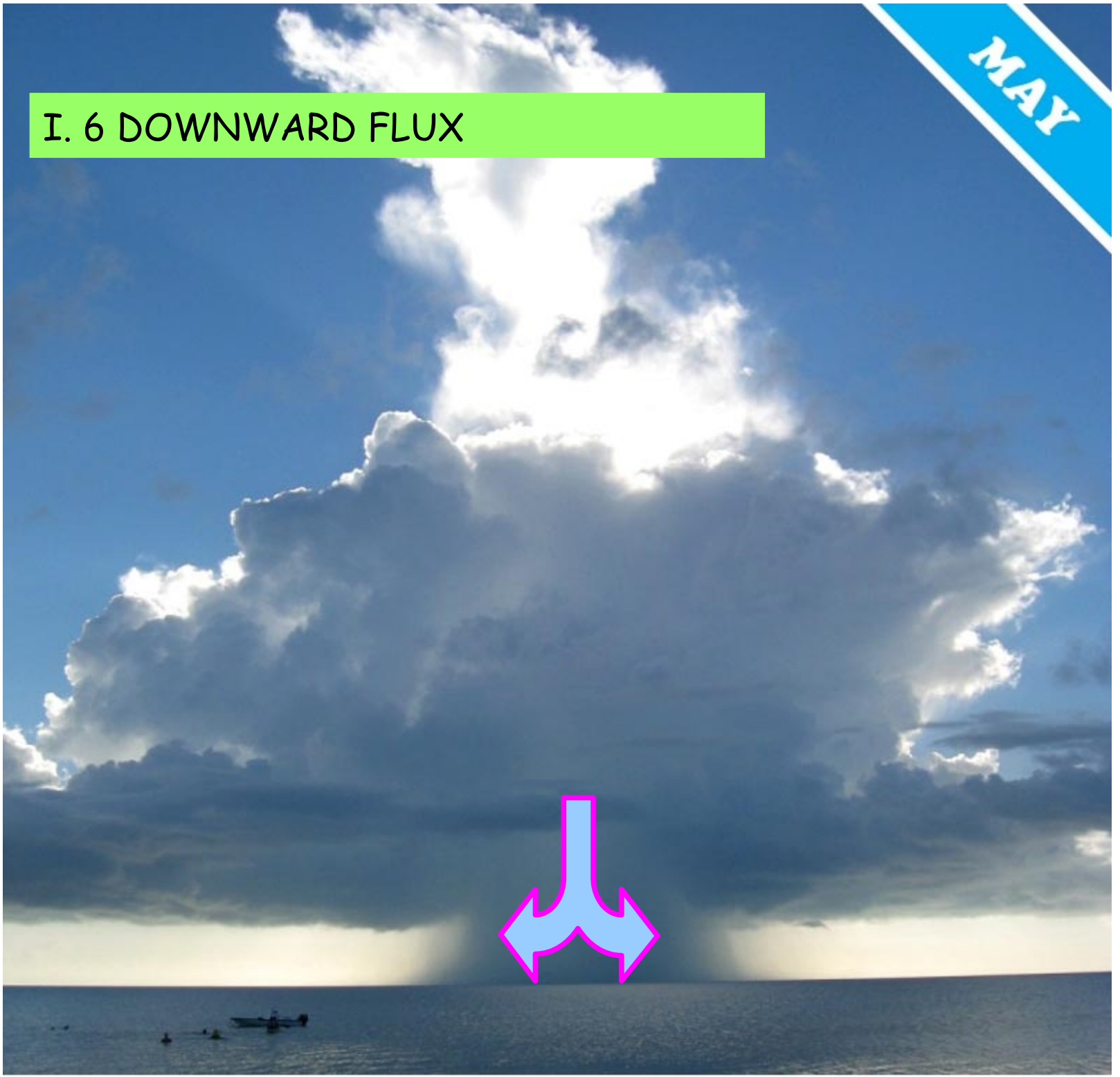

I. 6 VORTICES IN THE ABL

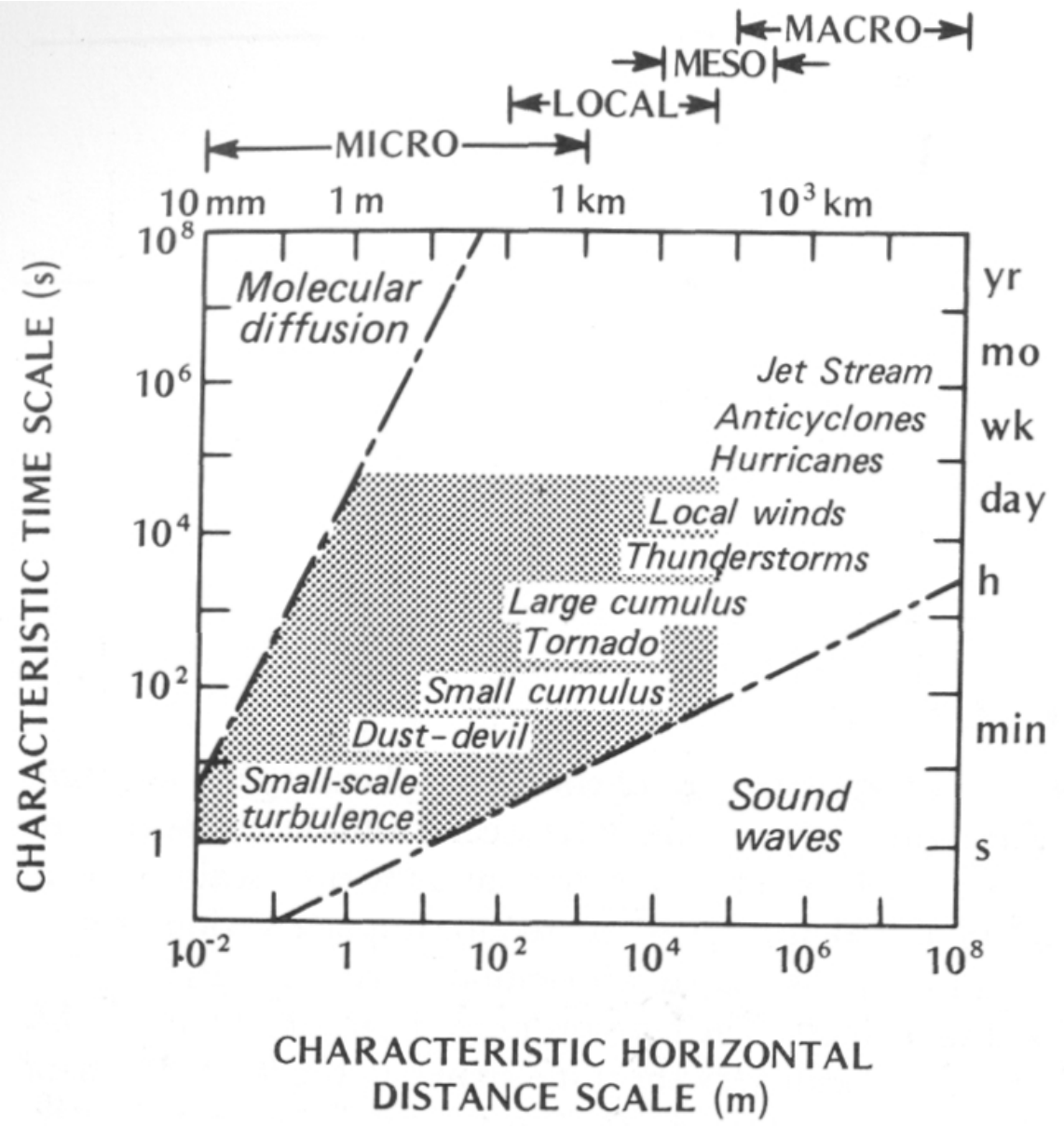

Figure 1.1 Time and space scales of various atmospheric phenomena. The shaded area represents the characteristic domain of boundary layer features (modified after Smagorinsky, 1974).

II Turbulence
II.1 Wind instruments used at SIRTA

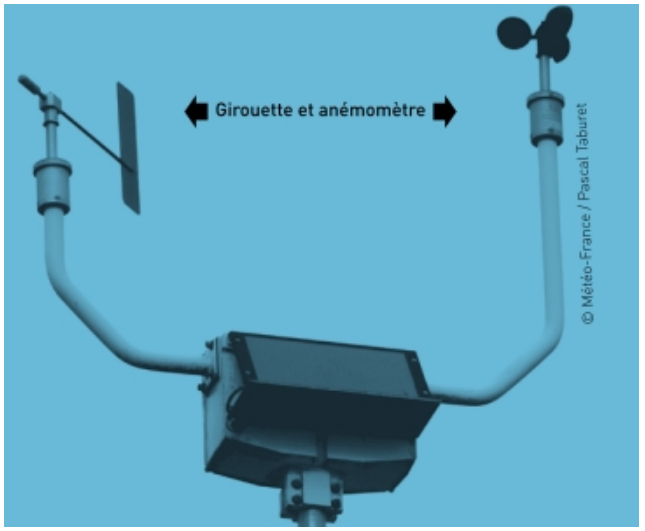

In situ,

- Cup anemometer
- Sonic anemoter
- Hot wire

Teledetection

- Wind lidar
- Sodars
- UHF and VHF profiler

THE ACARR WIND PROFILER IN KOCHI INDIA

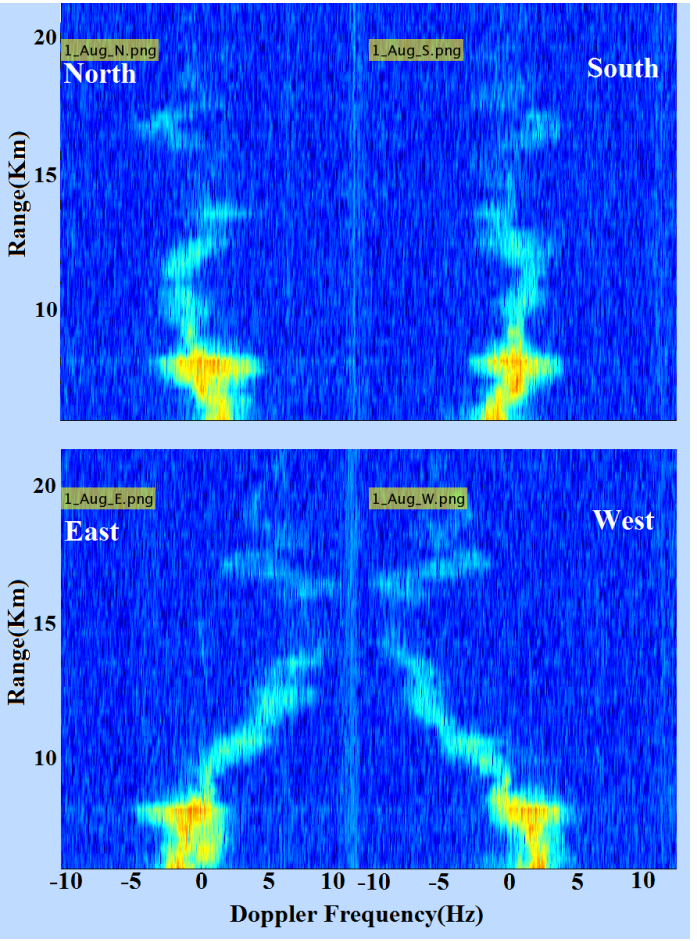

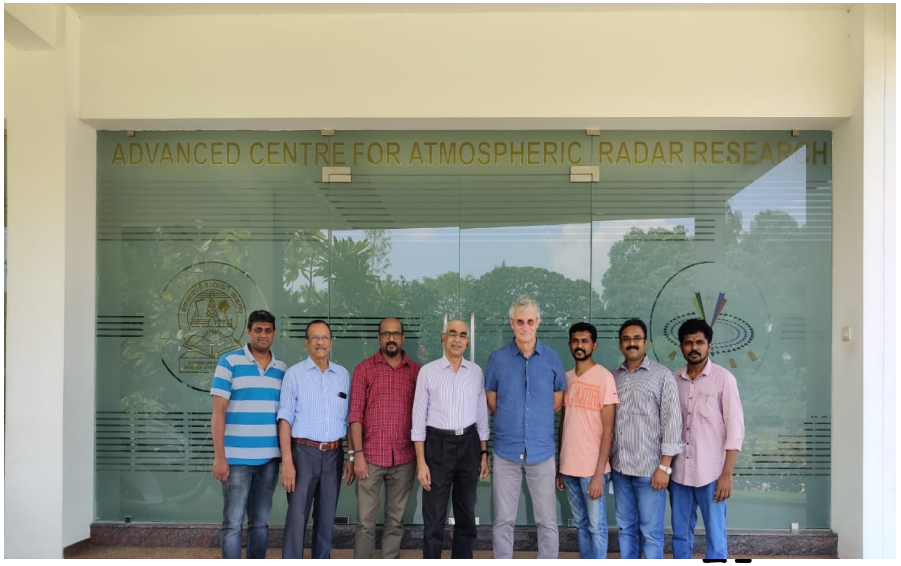

II.2 Turbulence scales

REYNOLDS NUMBER

Navier-Stokes equation

$$\frac{\partial \boldsymbol{u}}{\partial t} + \boldsymbol{u} \cdot \boldsymbol{\nabla} \boldsymbol{u} = -\frac{1}{\rho} \boldsymbol{\nabla} p + \nu \boldsymbol{\nabla}^2 \boldsymbol{u}$$

Scales $\nu = 10^{-5}\,\mathrm{m^2 s^{-1}}$ $U = 1 - 10\,\mathrm{ms^{-1}}$ $L = 1 - 10\,\mathrm{km}$

Reynolds number $\mathrm{Re} = \frac{|\boldsymbol{u} \cdot \boldsymbol{\nabla} \boldsymbol{u}|}{|\nu \boldsymbol{\nabla}^2 \boldsymbol{u}|} = \frac{U^2/L}{\nu U/L} = \frac{U L}{\nu}$

$\mathrm{Re} = 10^8 - 10^9$

Regime of developded turbulence for very large Re,
when dissipation is negligible et inertial effects dominate

Very close to the surface, U et L tend to 0 and the Reynolds as well.
There is very thin layer (of a few cm) just above the surface where viscosity dominates but above this layer viscosity can be neglected.

TURBULENCE

II.3 Statistical description of turbulence

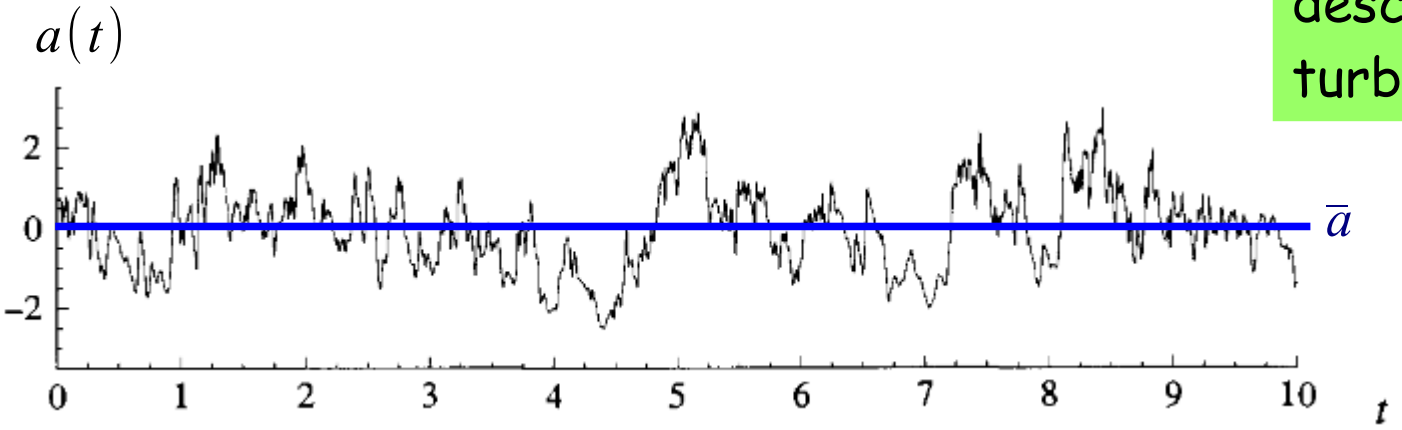

$a = \bar{a} + a'$ properties $\bar{\bar{a}} = \bar{a}$ $\bar{a'} = 0$

mean
- temporal
- spatial
- ensemble

Random fluctuations

Mean energy $\bar{e} = \frac{1}{2}\sum_i \overline{u_i^2} = \frac{1}{2}\sum_i \overline{(\bar{u}_i + u'_i)^2} = \frac{1}{2}\sum_i \overline{\bar{u}_i^2 + 2\bar{u}_i u'_i + u'^2_i} = \frac{1}{2}\sum_i \left(\bar{u}_i^2 + 2\bar{u}_i\bar{u'}_i + \overline{u'^2_i}\right)$

$$\bar{e} = \frac{1}{2}\sum_i \bar{u}_i^2 + \frac{1}{2}\sum_i \overline{u'^2_i}$$

Kinetic energy of t the mean flow

Turbulent kinetic energy E

COVARIANCES ET TEMPORAL CORRELATIONS

We consider quadratic quantities like $\overline{u'^2}, \overline{u'T'}, \overline{u'v'}$

Definition $\overline{u'T'}(t) = \int\int\int u'(\boldsymbol{x},t)\,T'(\boldsymbol{x},t)\,d^3\boldsymbol{x}$

Auto-covariance of a : $C_a(t,\tau) = \overline{a'(t)\,a'(t+\tau)} = \int\int\int a'(\boldsymbol{x},t)\,a'(\boldsymbol{x},t+\tau)\,d^3\boldsymbol{x}$

The rationale of such quantities is that a turbulent flow cannot be reproduced identically but its statistical properties are reproducible.

Stationarity when $C_a(t,\tau)$ depends only on τ.

Correlation $R_a(\tau) = \dfrac{C_a(\tau)}{C_a(0)}$

Integral time $I_a = \int_0^\infty R_a(\tau)\,d\tau$

This quantity is an estimate of the memory time of the flow.

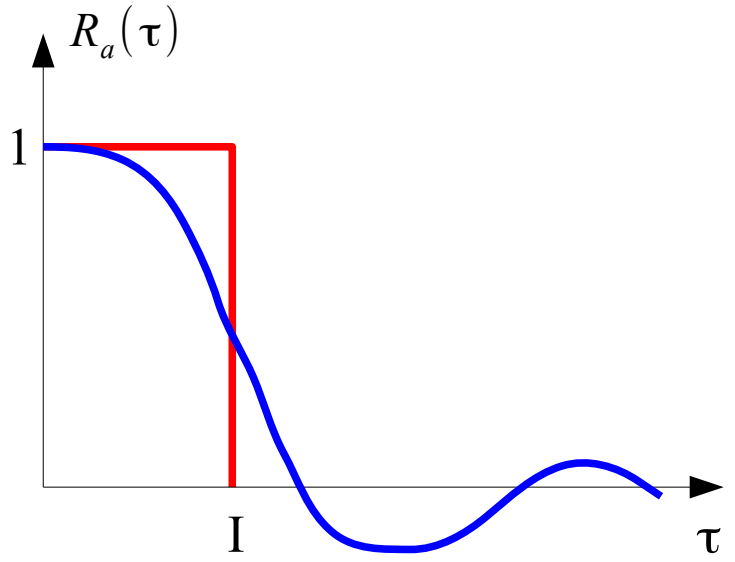

FOURIER ANALYSIS OF THE TURBULENT SIGNAL (in time or space)

In time

$$P_a(\omega)=\frac{1}{2\pi}\int_{-\infty}^{\infty} C_a(\tau)e^{-i\omega\tau}d\tau \qquad \text{et} \qquad C_a(\tau)=\int_{-\infty}^{\infty} P_a(\omega)e^{i\omega\tau}d\omega$$

In space

$$S_a(\boldsymbol{k},\boldsymbol{x})=\frac{1}{(2\pi)^3}\int\int\int C_a(\boldsymbol{\delta},\boldsymbol{x})e^{-i\boldsymbol{\delta}\cdot\boldsymbol{k}}d^3\boldsymbol{\delta}$$

Here $C_a(\boldsymbol{\delta},\boldsymbol{x})=\int_{-\infty}^{\infty} a(\boldsymbol{x},t)a(\boldsymbol{x}+\boldsymbol{\delta},t)dt$

In the sequel $\overline{f}$ means an average over time or space.

Statistical homogeneity when $\overline{a'(\boldsymbol{x})a'(\boldsymbol{x}+\boldsymbol{\delta})}$ and S_a do not depend on $\boldsymbol{x}$ but only on $\boldsymbol{\delta}$.

Isotropy if S_a depends only of the modulus of the wavenumbe $\boldsymbol{k}$ and not of its orientation: $S_a(\boldsymbol{k})=S_a(k)$.

The turbulent variance is then $E_a=\int_0^{\infty} E_a(k)dk$ where $E_a(k)=4\pi k^2 S_a(k)$

We denote $E(k)$ the turbulent kinetic energy per wavenumber k in the homogeneous isotropic case.

TURBULENCE SCALES

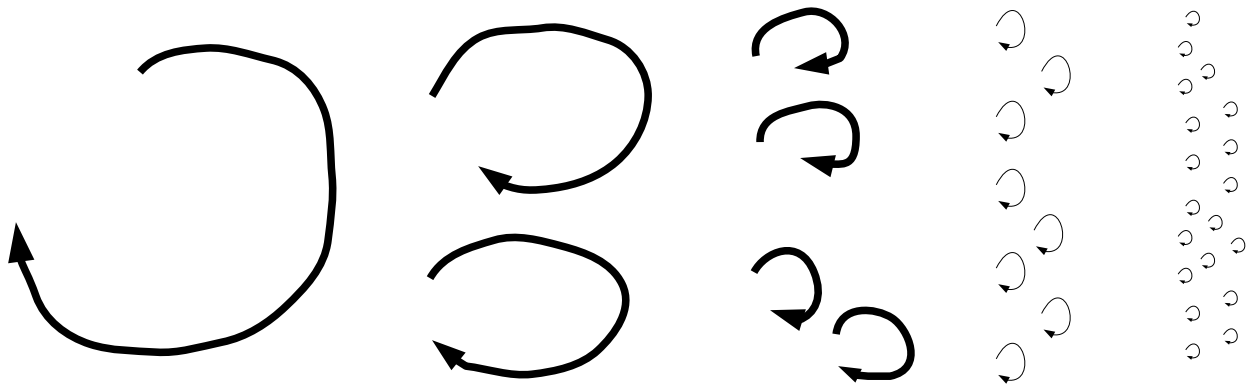

Richardson cascade
Kinetic energy is produced or injected at some macroscopic scale (convective rolls, clouds, nuages) and generate large eddies at the scale L0. Then these eddies break into smaller eddies, and the new eddies break into still smaller ones and so on until the scale reaches a few mm where the molecular dissipative forces are no longer negligible.

The quation for kinetic energy, $e=\frac{1}{2}\boldsymbol{u}^2$, is obtained by multiplying e Navier-Stokes equation by $\boldsymbol{u}$:

$$\frac{\partial}{\partial t}e+\nabla\cdot(\boldsymbol{u}\,e)=-\frac{1}{\rho}\cdot\nabla\cdot\boldsymbol{u}\,p+\nu\boldsymbol{u}\cdot\nabla^2\boldsymbol{u}$$

Energy flux, responsible of the transfer towards the small scales

Work of pressure forces

Viscous dissipation

II.4 TURBULENT CASCADE AND KOLMOGOROV LAW

u_l velocity $l=\frac{1}{k}$

difference at scale l

$$u_l \sim (l\,\epsilon)^{1/3} \sim u_{L_0}\left(\frac{l}{L_0}\right)^{1/3}$$

R_l Reynolds number at scale l

$$R_l = \frac{l\,u_l}{\nu} = R_{L_0}\left(\frac{l}{L_0}\right)^{4/3}$$

R_{L_0} Reynolds number of the flow

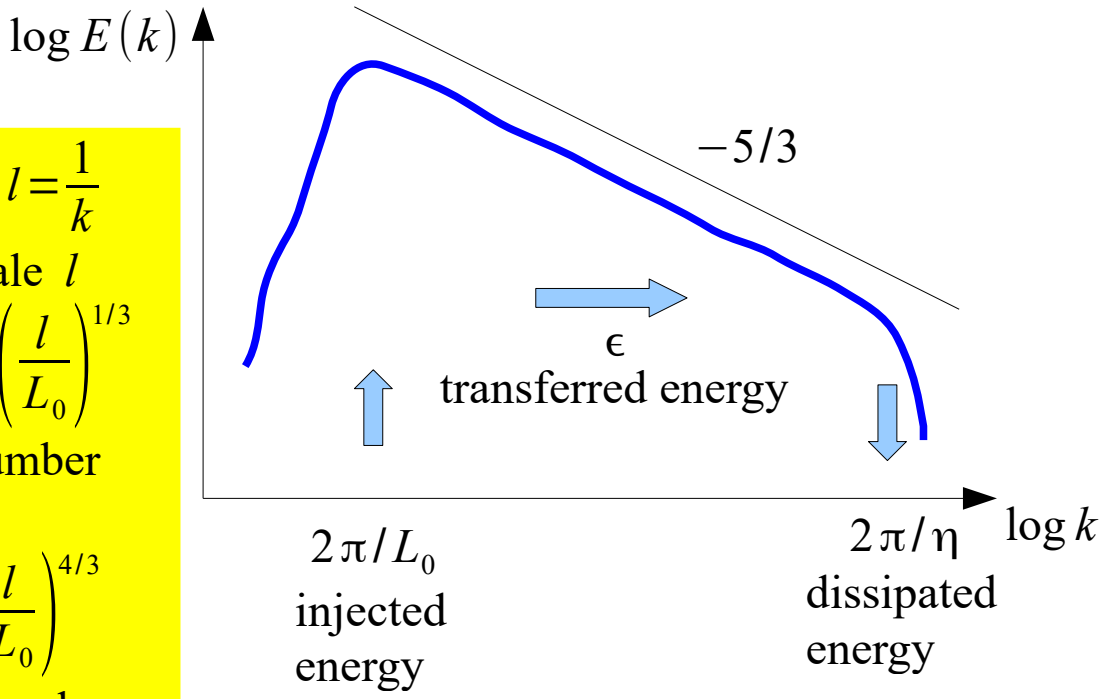

η dissipation scale

$$\eta = \nu^b \epsilon^a$$

$$[\nu] = L^2 T^{-1}$$

$$[\epsilon = \frac{dE}{dt}] = L^2 T^{-3}$$

$$[\nu^b \epsilon^a] = L^{2a+2b} T^{3a+b} = L$$

hence $a=-1/4$ et $b=3/4$

$$\eta(\epsilon,\nu) = \left(\frac{\nu^3}{\epsilon}\right)^{1/4}$$

η also obtains by setting $R_\eta = 1$

such that $u_\eta = (\eta\epsilon)^{1/3} = \frac{\nu}{\eta}$

Then $\eta = L_0 R_{L_0}^{-3/4}$

In a stationary regime

ϵ : injected energy rate, dissipated energy, energy flux across scales within the cascade.

$[E(k)] = L^3 T^{-2}$ et $E(k)$ depends only of ϵ and k, not of de ν, hence the Kolmogorov law

$$E(k) = C\,\epsilon^{2/3} k^{-5/3}$$

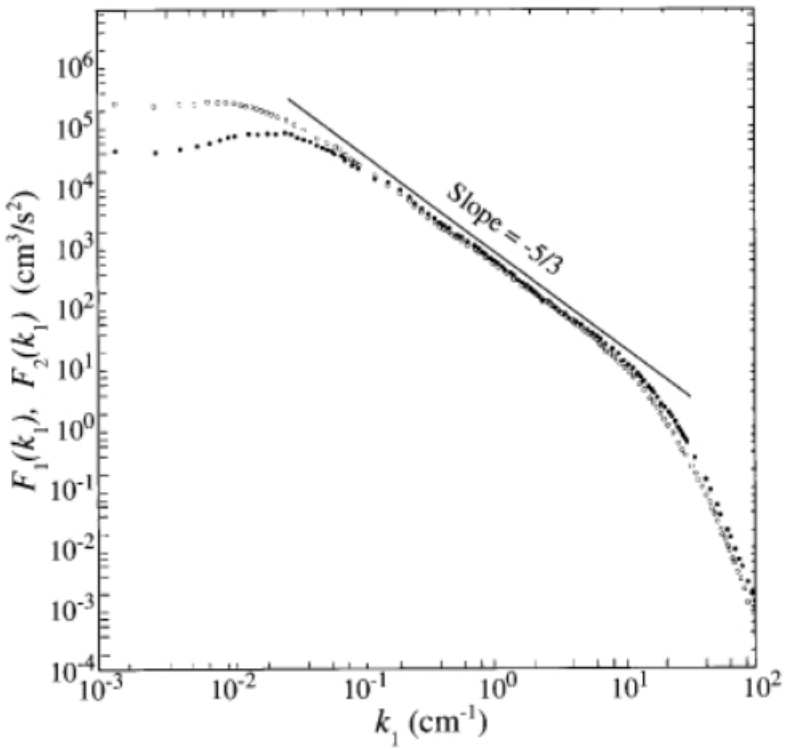

Fig. 5.7. log–log plot of the energy spectra of the streamwise component (white circles) and lateral component (black circles) of the velocity fluctuations in the time domain in a jet with $R_\lambda = 626$ (Champagne 1978).

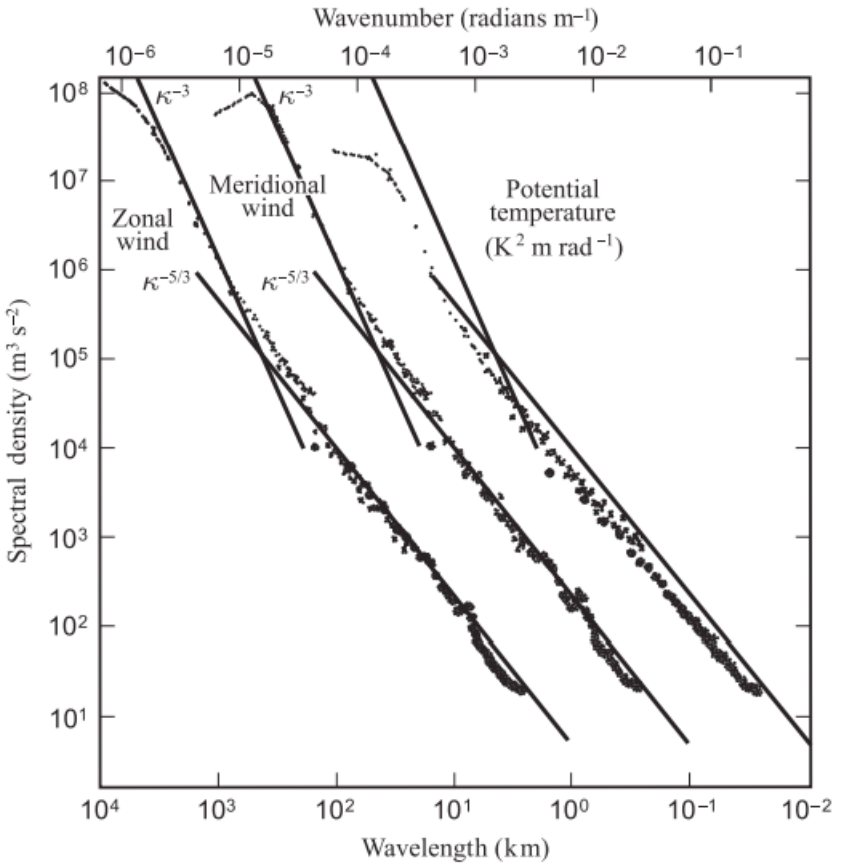

Figure 7.6 Spectra of horizontal velocity components and temperature in the upper atmosphere. From Nastrom and Gage (1985).

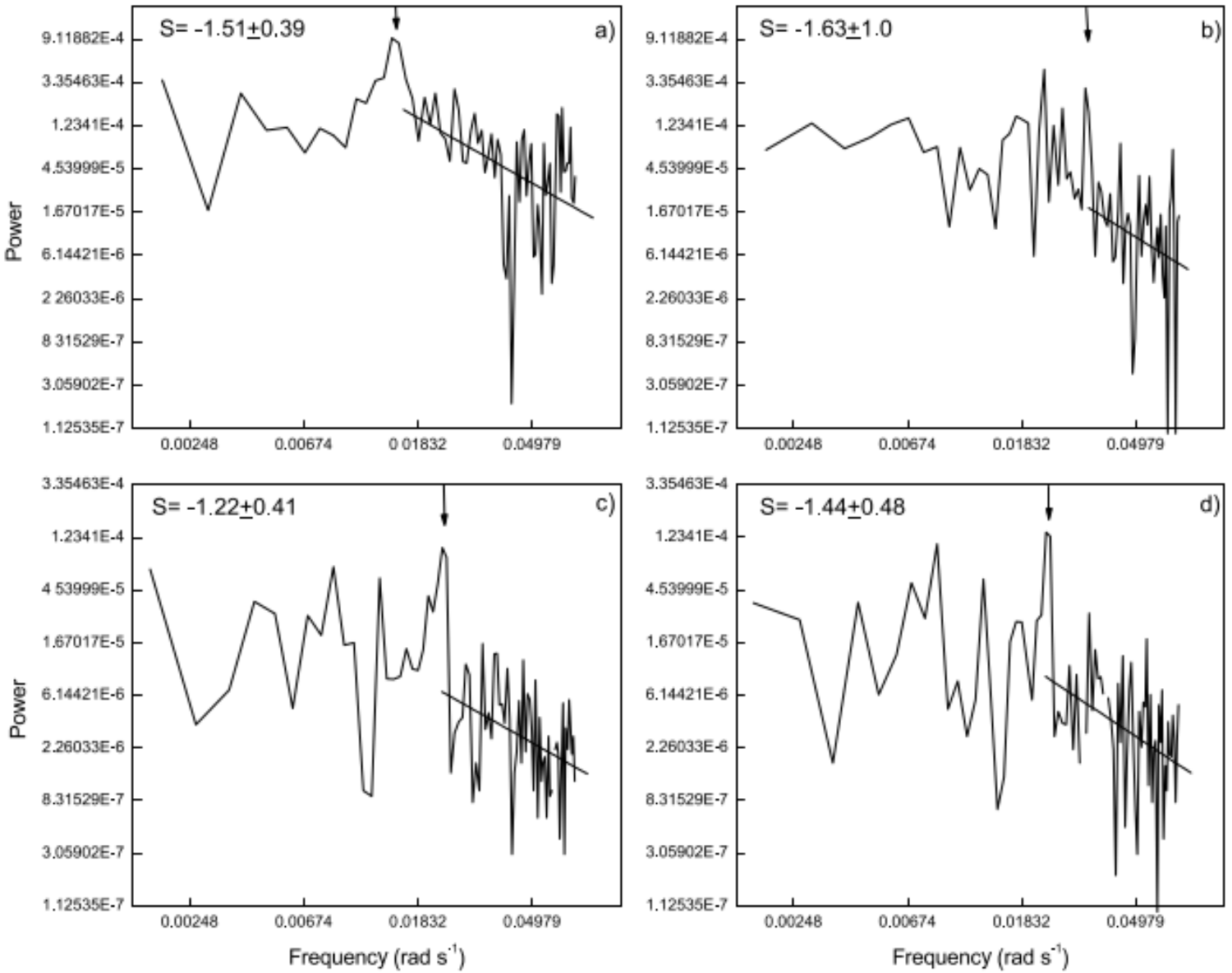

Figure 2. Typical temporal spectra of vertical wind. (a) 29 January at 9.9 km. (b) 29 January at 19.95 km. (c) 26 February at 6.3 km. (d) 26 February at 6.45 km. The value of the slope *S* is indicated in each diagram. *N* is indicated by a downward arrow.

II.5 TURBULENT FLUXES

Temperature equation (far from sources and neglecting dissipation)

$$\frac{\partial \theta}{\partial t} + \nabla \cdot \boldsymbol{u}\theta = 0$$

Mean temperature equation

$$\frac{\partial \bar{\theta}}{\partial t} + \nabla \cdot \bar{\boldsymbol{u}}\bar{\theta} + \nabla \cdot \overline{\boldsymbol{u}'\theta'} = 0$$

Mean flow divergence

Turbulent flux divergence

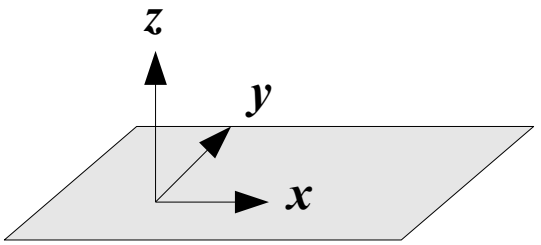

surface

$$\nabla \cdot \overline{\boldsymbol{u}'\theta'} = \frac{\partial}{\partial x}\overline{u'\theta'} + \frac{\partial}{\partial y}\overline{v'\theta'} + \frac{\partial}{\partial z}\overline{w'\theta'}$$

Homogeneous case in x and y

The instantaneous flow is not invariant in x and y but the statistical properties are invariant

II.6 Turbulent fluxes and Ekman layer
Surface jet

- Due to the equilibrium between friction and Coriolis force, the Ekman theory predicts that the surface wind is rotated by 45° with respect rapport to its direction in the free atmosphere. In practice, instabilities limit this rotation.

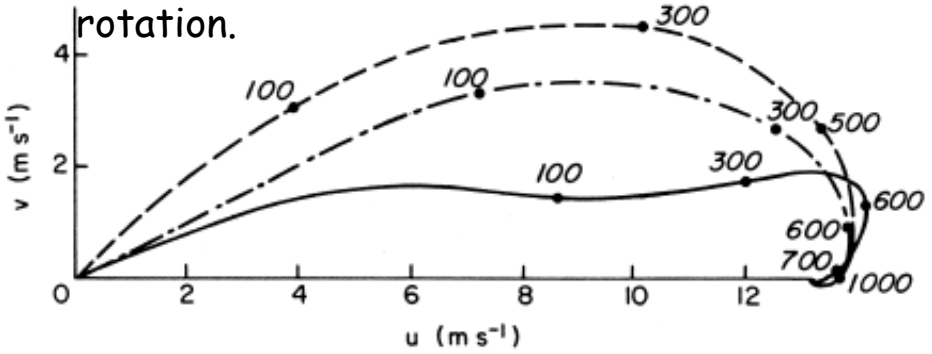

Holton

This phenomenon is also responsible of the formation of the nocturnal jet a few hundred m above ground when friction is reduced at night. The wind speed can then approach (by inertial oscillation) the free atmosphere wind.

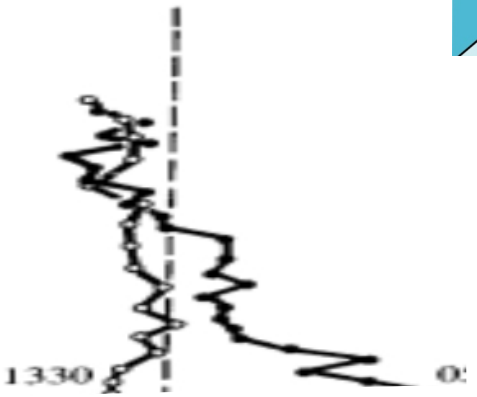

- The Ekman rotation is an important process in the ocean. It explains the angle between the surface wind and the induced current. This is important to explain the upwellings in coastal regions.

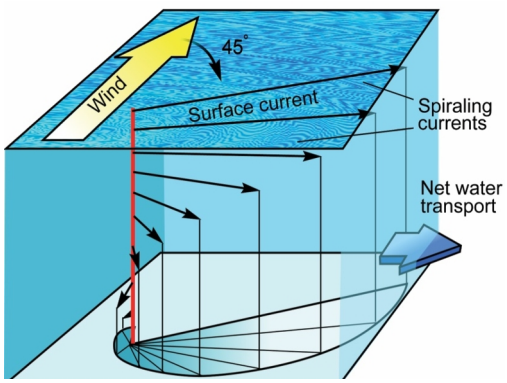

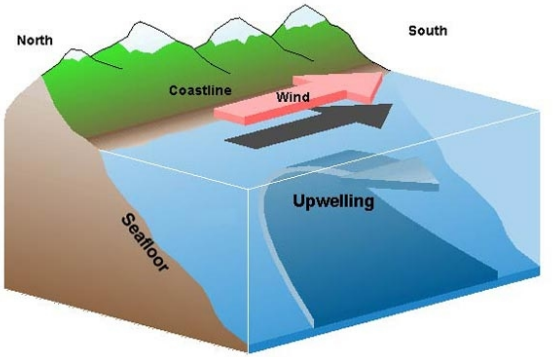

Viscous Ekman layer

The equations for a viscous Ekman layer are

$$\frac{\partial}{\partial t}\bar{u}+f(v_g-\bar{v})-\nu_T\frac{\partial^2\bar{u}}{\partial z^2}=0$$

$$\frac{\partial}{\partial t}\bar{v}-f(u_g-\bar{u})-\nu_T\frac{\partial^2\bar{v}}{\partial z^2}=0$$

Here, we assume for simplicity, that turbulence leads to augmented viscosity denoted as ν_T. Wrong but useful.

Boundary conditions are $\bar{u}(0)=\bar{v}(0)=0$ et $\bar{u}(\infty)=u_g, \bar{v}(\infty)=v_g$

To simplify, we assume that the geostrophic wind is aligned with x, thus $v_g=0$.

The equations can be easily solved using complex velocity $c=\bar{u}+i\bar{v}$ and we have:

$$\frac{\partial c}{\partial t}-if(u_g-c)=\nu\frac{\partial^2 c}{\partial z^2}$$

The stationary solution satisfies $if(c-u_g)=\nu\frac{\partial^2(c-u_g)}{\partial z^2}$ hence $c=u_g+ae^{-(1+i)\frac{z}{\delta}}$

with $\delta=\sqrt{\frac{2\nu}{f}}$. The bottom boundary condition provides $c=u_g\left(1-e^{-(1+i)\frac{z}{\delta}}\right)$,

that is $\bar{u}=u_g\left(1-e^{\frac{-z}{\delta}}\cos\frac{z}{\delta}\right)$ and $\bar{v}=u_g e^{\frac{-z}{\delta}}\sin\frac{z}{\delta}$

Hodograph of u

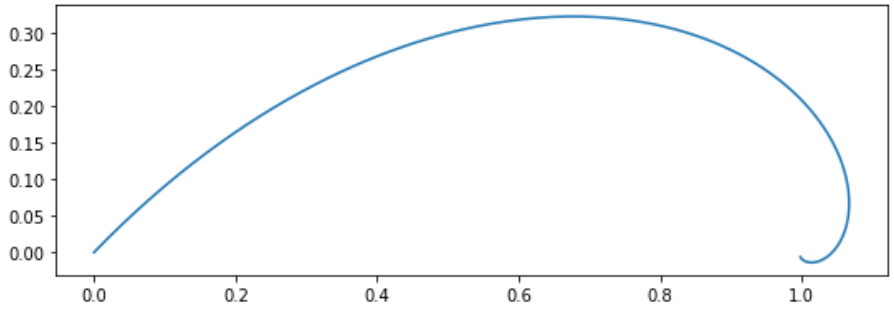

Inertial oscillations

The equations without diffusion is:

$$\frac{\partial c}{\partial t} - if(u_g - c) = 0$$

The time dependent solution is

$$c(t) - u_g = (c(0) - u_g)e^{-ift}$$

In other words, the velocity vectors follows a circle around the geostrophic wind. The full rotation is performed in 1day/sin(latitude).

Such oscillation are most easily observed in the polar regions where they are the fastest.

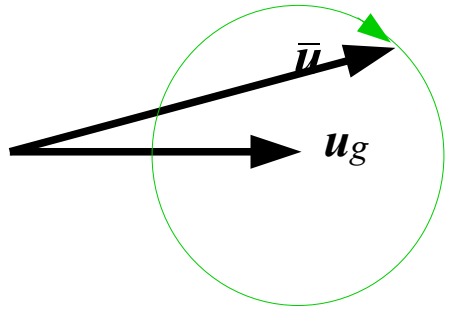

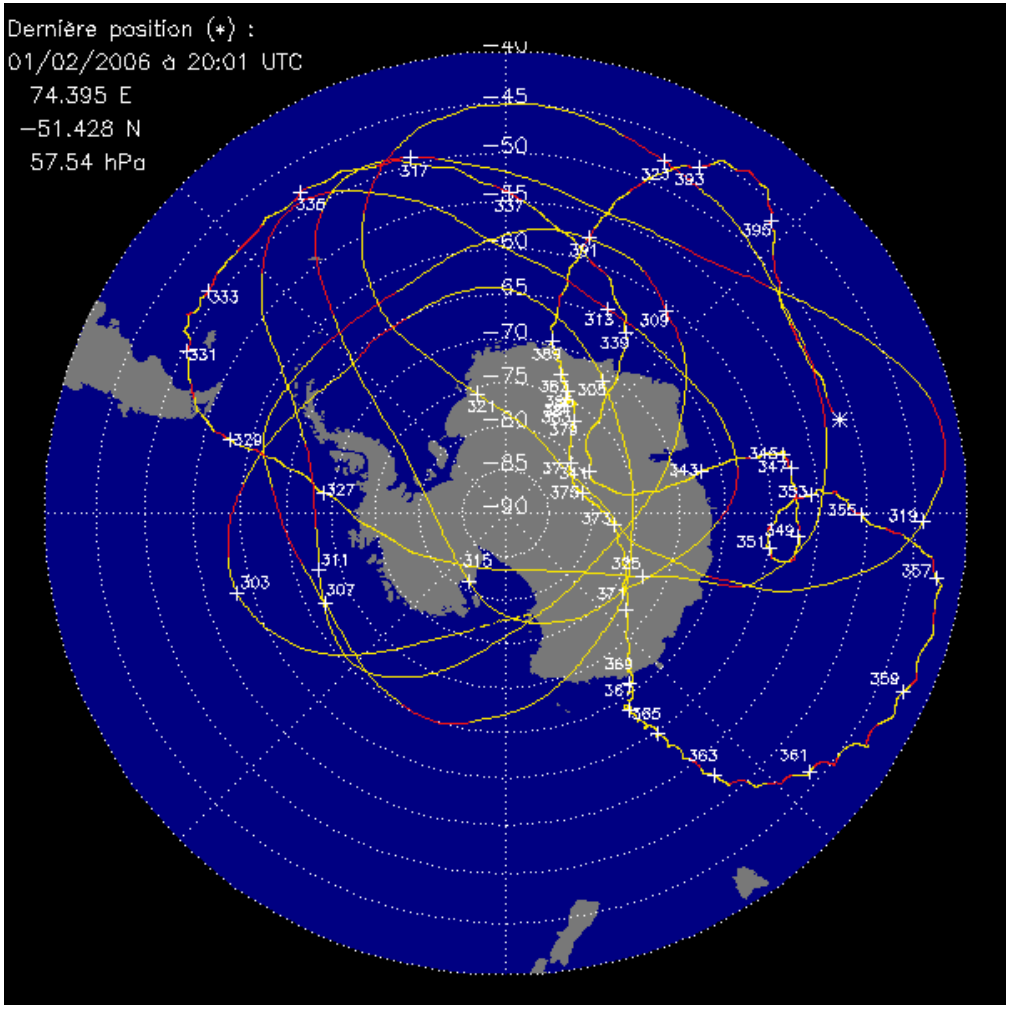

Nocturnal jet at the top of the ABL

Ekman layer equations with momentum turbulent flux

$$\frac{\partial}{\partial t}\bar{u} + f\left(v_g - \bar{v}\right) + \frac{\partial}{\partial z}\overline{u'w'} - \nu\frac{\partial^2 \bar{u}}{\partial z^2} = 0$$

$$\frac{\partial}{\partial t}\bar{v} - f\left(u_g - \bar{u}\right) + \frac{\partial}{\partial z}\overline{v'w'} - \nu\frac{\partial^2 \bar{v}}{\partial z^2} = 0$$

The viscous term is negligible. The flux vanishes during the night (stable ABL). During the day, the flux constrains a stationary response.

The turbulents fluxes are big with respect to the viscous terms in these equations. The divergence of the momentum flux exerts a drag on the flow. The problem is to make this effect a function of the profiles $\bar{u}(z)$ and $\bar{v}(z)$.

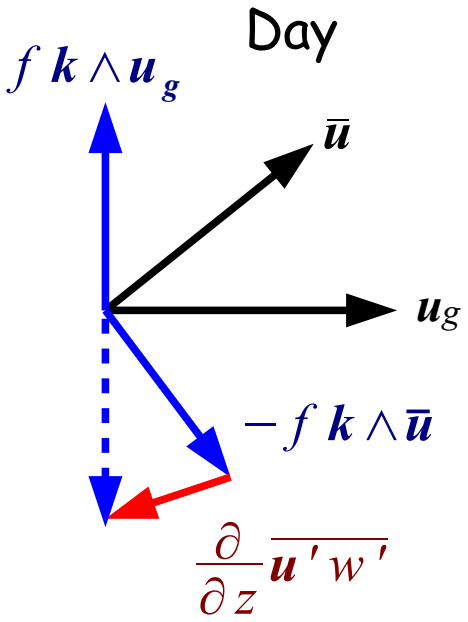

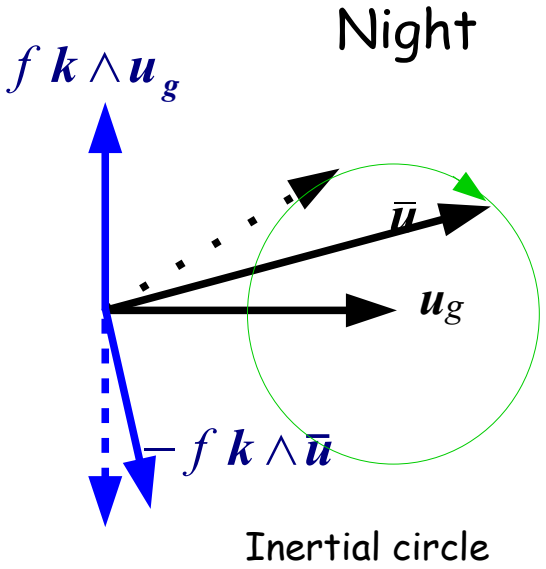

When friction is large (diurnal mixed layer), the wind is equilibrated via the Coriolis force with pressyre and drag. When friction is small (during night), the equilibrium is broken and the wind follows and inertial circle around the geostrophic wind [nocturnal jet]

NOCTURNAL JET

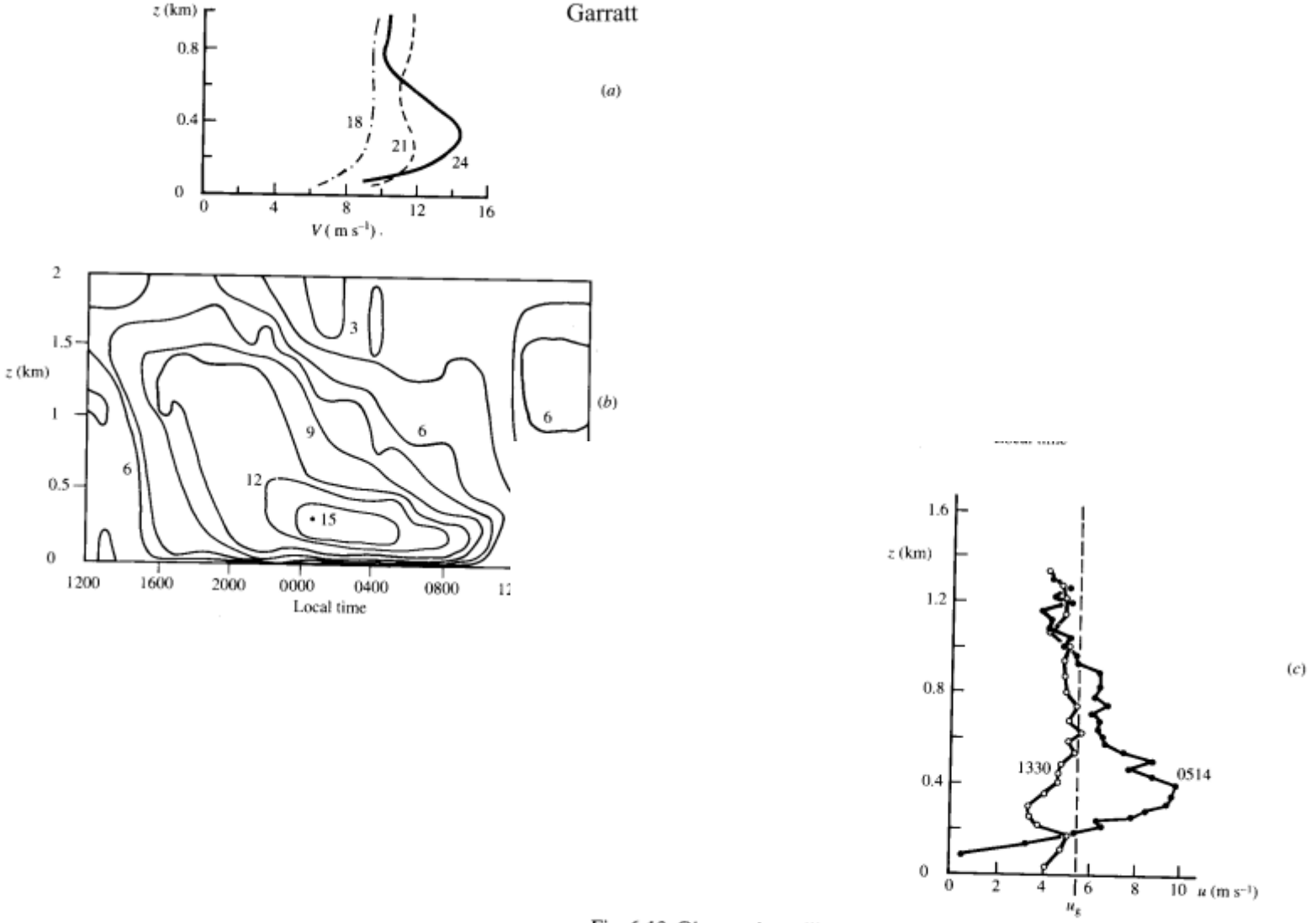

Fig. 6.18 Observations illustrating the formation of the nocturnal jet. (*a*) Wind-speed profiles on day 13 of WANGARA, local times indicated. (*b*) Height–time cross-section of wind speed (in $m\,s^{-1}$) on days 13/14 at WANGARA. Isopleths of wind speed are drawn at $1.5\,m\,s^{-1}$ intervals. (*c*) Profiles of the u-component of the wind velocity, with the x-axis along the geostrophic wind direction, for mid-afternoon (1330 UT, 6 August, 1974) and early morning (0514, 7 August, 1974) near Ascot, England. After Thorpe and Guymer (1977), *Quarterly Journal of the Royal Meteorological Society*.

Low level jet
two mechanisms

- Generation by intertial relaxation when the nocturnal temperature inversion (stable BL) and the reduction of momentum drag decouple the surface from the top of the boundary layer ; The flow can then become supergeostrophic.
-

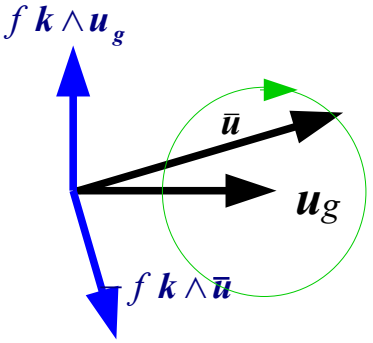

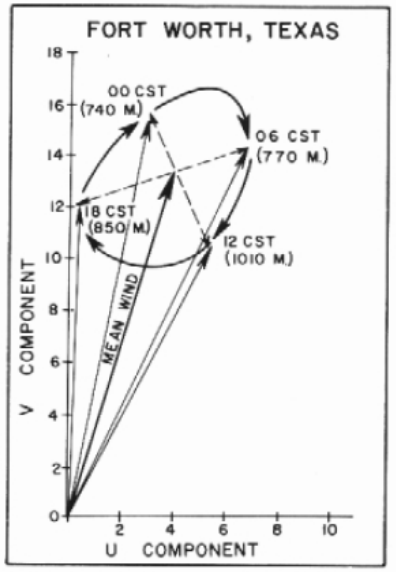

Formation of a large scale slope wind that satisfies the thermal wind relation in response to the temperature gradient along the slope of the Great Plains. Suppression of the diurnal component by the boundary layer.

day

night

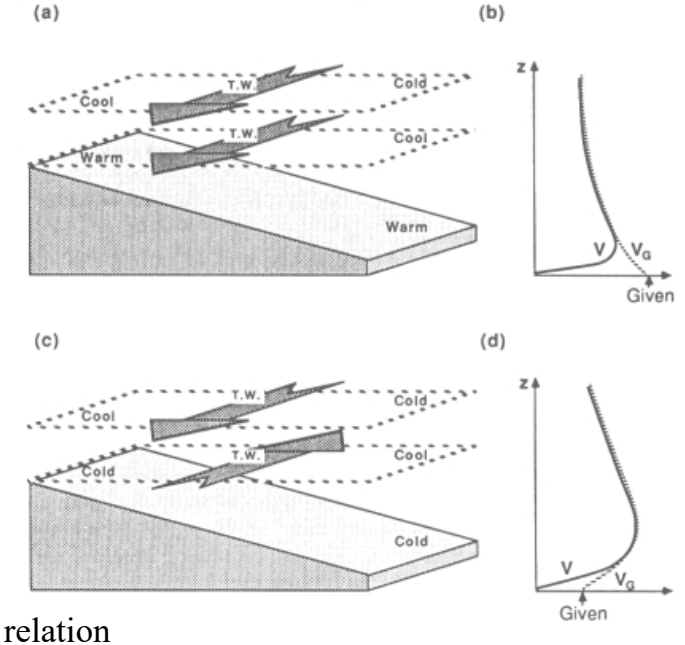

Thermal wind relation

$$\frac{\partial \vec{u}_g}{\partial z}=\frac{g}{f\bar{T}}\vec{k}\wedge\vec{\nabla}\bar{T}$$

where $f=2\Omega\sin(\text{latitude})$

$\vec{k}$: unit vertical vecto

II.7 MIXING LENGTH

The mixing length theory is the simplest one to relate the turbulent fluxes to the characteristics of the mean flow

The turbulent flux of a associated to the displacement of the parcel is

$$\overline{w'a'} = \overline{w'_u a'_u} + \overline{w'_d a'_d}$$

w'_u and w'_d are the velocity fluctuations towards up and down directions.

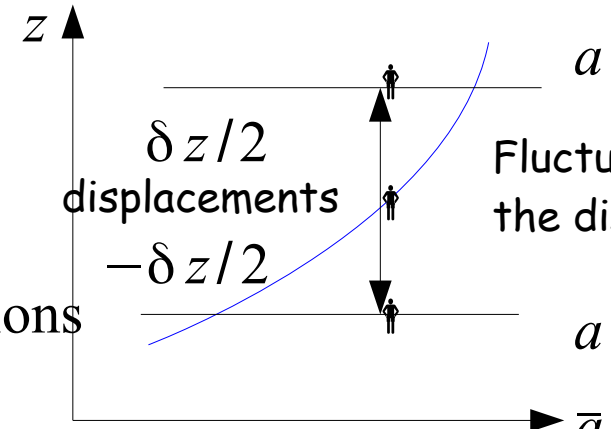

$$a'_u = \frac{-\delta z}{2}\frac{\partial \bar{a}}{\partial z}$$

Fluctuation of a due to the displaced parcel

$$a'_d = \frac{\delta z}{2}\frac{\partial \bar{a}}{\partial z}$$

Assuming that the velocity fluctuation has a characteristic value $|w'_u| = |w'_d| = W$

then $\overline{w'a'} = 2 \times \frac{-W\delta z}{2}\frac{\partial \bar{a}}{\partial z} = -K_a \frac{\partial \bar{a}}{\partial z}$ and $\frac{\partial}{\partial z}\left(\overline{w'a'}\right) = \frac{-\partial}{\partial z} K_a \frac{\partial \bar{a}}{\partial z}$

where K_a is a turbulent diffusivity or viscosity.

it remains to determine the mixing length δz.

If $\delta z \approx 1000\,\text{m}$ and $W = 1\,\text{m/s}$, then $K_a = 500\,\text{m}^2/\text{s}$.

The total flux (turbulent + molecular)

$$\overline{w'a'} - \nu \frac{\partial \bar{a}}{\partial z}$$

is

$$-(K_a + \nu)\frac{\partial \bar{a}}{\partial z}$$

Pipe flow

At the center of the pipe $K_a \gg \nu$

The turbulent profile (grand Re) is much flatter than the laminar profile for the same pressure gradient

because $0 = \frac{-1}{\rho}\frac{\partial p}{\partial x} + \frac{1}{r}\frac{\partial}{\partial r}\left(r(K_u + \nu)\frac{\partial \bar{u}}{\partial r}\right)$

(velocity equation in a cylindrical pipe in stationary regime

Velocity profile in a pipe

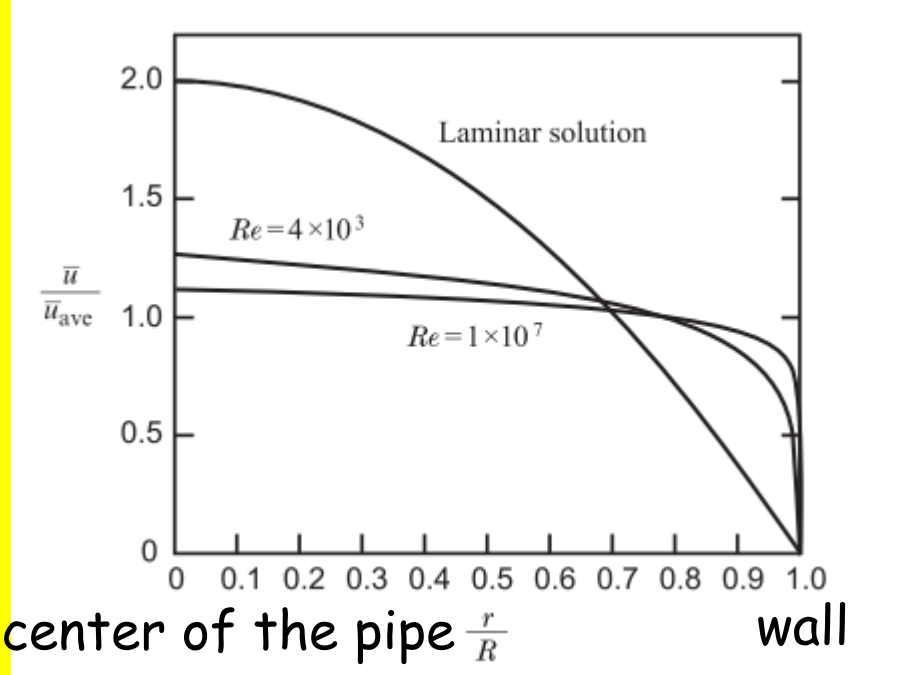

Wyngaard

K_u is not a constant because the turbulent profil is different from the laminar profile

At the wall, the turbulent flux vanishes because $w' \to 0$. There is a viscous layer where $\nu > K_u$. Above this layer, ν is negligible but the size of the main turbulent eddies is bounded by the distance to the wall.

This is the wall turbulent layer.

II.7 WALL TURBULENT LAW (LOGARITHMIC LAYER)

$\bar{u}(z)$ vertical profile of the horizontal velocity

Let us define $\tau(z)=\overline{u'w'}-\nu\frac{\partial \bar{u}}{\partial z}$ et $u_*^{\,2}=-\tau(0)=\nu\frac{\partial \bar{u}}{\partial z}(z=0)$. We admit that $\frac{\partial \tau}{\partial z}(z=0)=0$. Therefore, there is a layer near the wall (or the surface) such that $\tau\approx -u_*^{\,2}$.

Inside this layer, there is also a viscous sublayer which thickness is determined by the viscous scale $z_*=\frac{\nu}{u_*}$

and where $u(z)=u_*\frac{z}{z_*}$

Above that, for z small enough but $z\gg z_*$ is the domain of the wall law where the velocity gradient can only depend on u_* and z, implying

$$\frac{\partial \bar{u}}{\partial z}=\frac{u_*}{\kappa z}, \text{ hence } \bar{u}(z)=\frac{u_*}{\kappa}\ln\left(\frac{z}{z_0}\right)$$

where κ is denoted as the von Karman constant and z_0 is the surface rugosity.

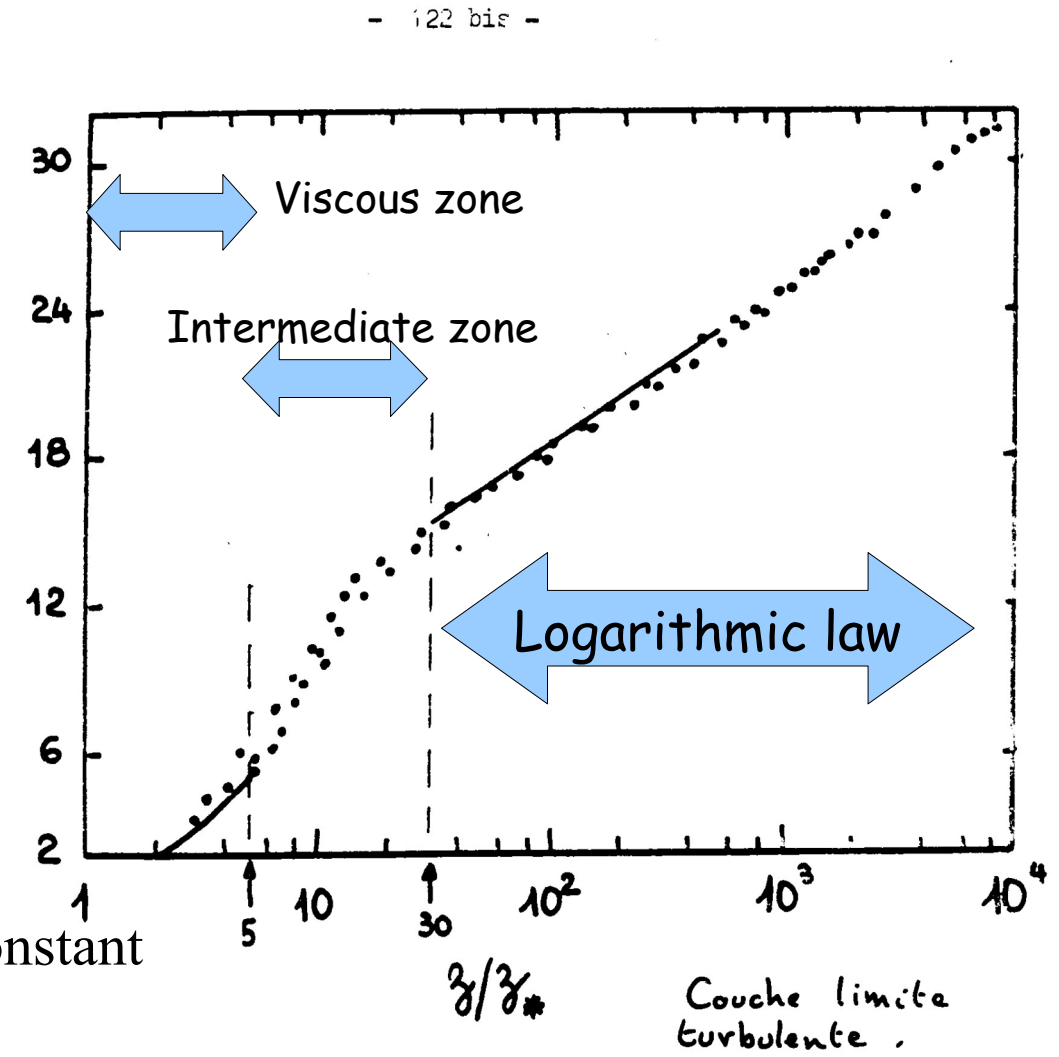

Surface turbulent layer rugosity

The rugosity has been defined as $u(z)=\frac{u_*}{\kappa}\log\left(\frac{z}{z_0}\right)$

It is often modified as $u(z)=\frac{u_*}{\kappa}\log\left(\frac{z+z_0}{z_0}\right)$

to have $u(0)=0$

	z_0
Icy surface	0.0001 m
Short grass	0.01 m
High grass	0.05 m
Pasture	0.20 m
Suburb	0.6 m
Forest, city	1-5 m

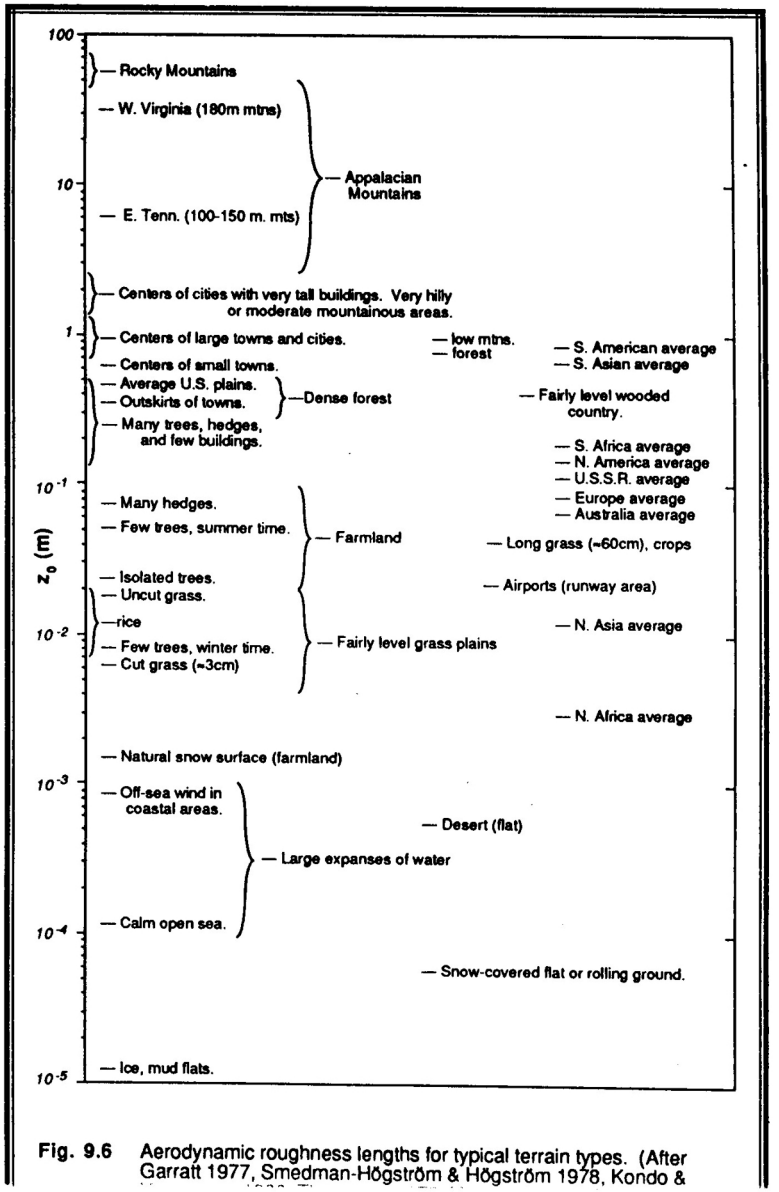

Fig. 9.6 Aerodynamic roughness lengths for typical terrain types. (After Garratt 1977, Smedman-Högström & Högström 1978, Kondo &

The logarithmic law is one type of the mixing length theory
where the mixing length is proportional to the distance to the wall

Taking $K_u = \kappa z u_*$, we get $u_*^2 = |\overline{u' w'}| = \left| -K_u \frac{\partial \bar{u}}{\partial z} \right| = \kappa u_* z \frac{\partial \bar{u}}{\partial z}$

In a wind tunnel, the thickness of the viscous sub-layer is of the order
of a few cm. That of the logarithmic law is of the order
of a few tens of m in the atmosphere .

The standard value of the von Karman constant is $\kappa \approx 0{,}4$
A typical value of u_* is $0{,}3$ m/s.

Surface turbulent layer rugosity above a canopy

$$\bar{u} = \frac{u_*}{\kappa} \log \frac{z-d}{z_0}$$

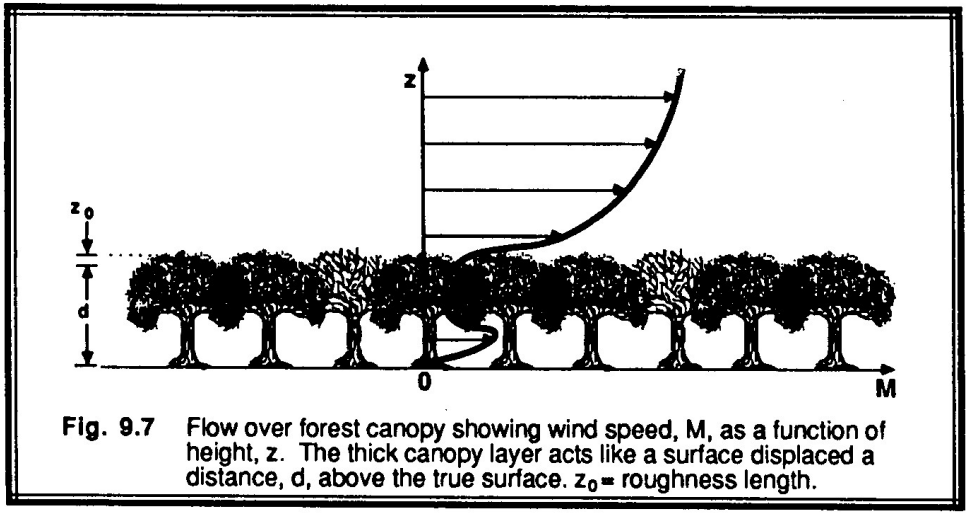

Fig. 9.7 Flow over forest canopy showing wind speed, M, as a function of height, z. The thick canopy layer acts like a surface displaced a distance, d, above the true surface. z_0 = roughness length.

Surface turbulent layer
rugosity above the sea

Above water, rugosity depends on the wind speed because the wind determines the state of the surface.

$$z_0 = \alpha \frac{u_*^2}{g} + 0.11 \frac{\nu}{u_*}$$

α is the Charnock parameter. Its standard value is 0,016 but some models let it depend on the propagating swell.

AERODYNAMIC FORMULA

$$-\rho_0 \overline{u'w'} = \rho_0 u_*^2 = \rho_0 C_{DN} \bar{u}^2(z_R)$$

with $z_R = 10\,\mathrm{m}$

Hence $C_{DN} = \dfrac{\kappa^2}{(\log(z_R/z_0))^2}$

Here we relate u* to the standard measurement of wind on a mast (or the bow of a boat) 10m above the surface.

Over water (where z_0 depends of u_*), empirical formula :

$$C_{DN} = (0{,}75 + 0{,}067\, u(z_R))\, 10^{-3}$$

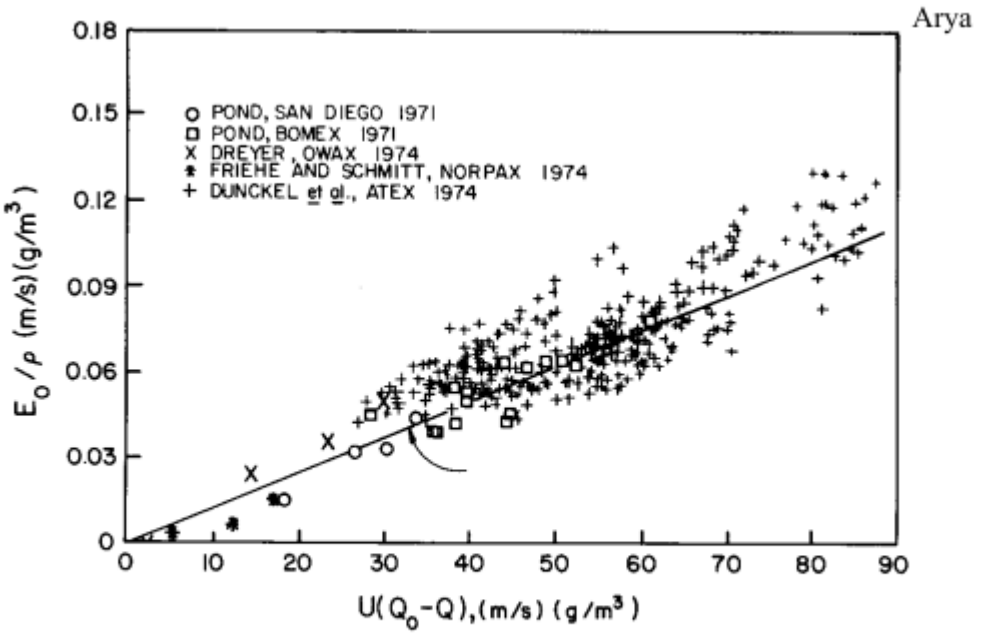

Fig. 13.6 Observed moisture flux at the sea surface as a function of $U(Q_0 - Q)$ compared with Eq. (13.8) with $C_w = 1.32 \times 10^{-3}$, indicated by the arrow. [After Friehe and Schmitt (1976).]

For a scalar a:

$a_* = \overline{w'a'}(z=0)/u_*$

et

$$\bar{a}(z) - \bar{a}(0) = \frac{-a_*}{\kappa} \log \frac{z}{z_{0a}}$$

Defining C_{aN} such that

$\rho_0 \overline{w'a'} = \rho_0 C_{aN}\, r\, u(z_R)(\bar{a}_0 - a(z_R))$

and $C_{aN} = \dfrac{\kappa^2}{\log \dfrac{z_R}{z_0} \log \dfrac{z_R}{z_{0a}}}$

II.8 STRATIFICATION OF THE ABL

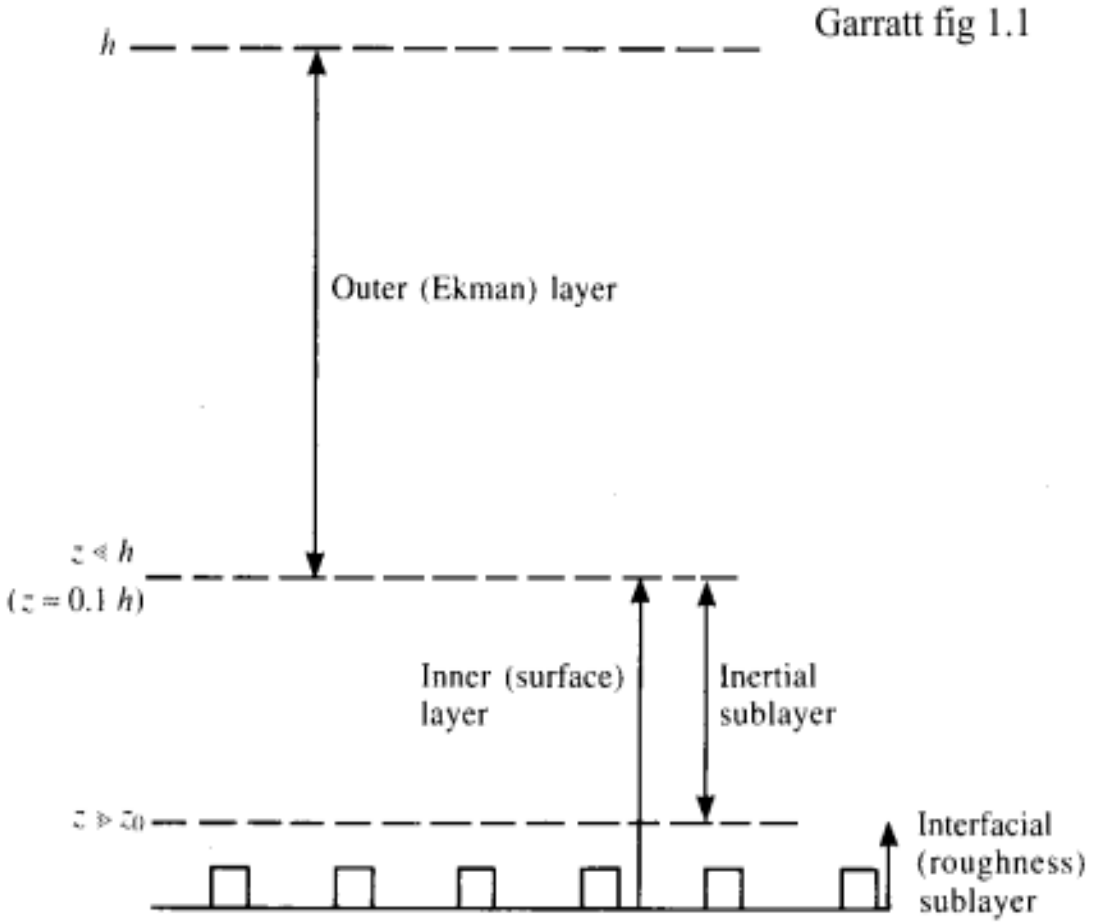

II.9 MONIN-OBUKHOV LENGTH

What has been done so far is valid in the neutral case or close to the neutral case where the effects of the thermal flux (or of buoyancy) can be neglected.

Now, if $b = g\frac{\theta'}{\theta_0}$, the Monin-Obukhov length is defined as $L = -\frac{u^{*3}}{\kappa\left(\overline{w'b'}\right)_S} = -\frac{u^{*3}\theta_0}{\kappa g\left(\overline{w'\theta'}\right)_S}$

where the indice S denotes the flux measured just above the rugosity height.

$Q_0 = \left(\overline{w'\theta'}\right)_S$ is thus the heat flux at the surface.

L is negative under unstable conditions $Q_0 > 0$

L is positive under stable conditions $Q_0 < 0$

L is infinite under neutral conditions $Q_0 = 0$

$|L|$ is large (several hundred of m) under windy and cloud covered conditions

Under sunny and calm conditions (nice summer day) L is of the order of -10m.

Under stable nocturnal and calm conditions, L is positive of the order of a few tens to a hundred m

The conditions are neutral or quasi-neutral for $z \ll |L|$, that is very close to the surface.

The condition $z \gg |L|$ are favored when L is small enough in absolute value, that is under calm air, then the momentum flux u^* is small and the ABL is determined by the heat flux .

Furthermore if $L < 0$, free convection and mixing homogeneisation occur.

SIMILARITY THEORY OF MONIN-OBUKHOV
(generalization of the log-law)

Assuming that the turbulence properties in the ABL depend only

of z, u^*, Q_0 and of the buoyancy parameter $\frac{g}{\theta_0}$, it can be shown (Pi theorem of Buckingham)

that all quantities adimensionnalized by these parameters is a function of $\frac{z}{L}$.

We the define the functions ϕ_m and ϕ_h such that

$$\frac{\kappa z}{u^*}\frac{\partial \bar{u}}{\partial z}=\phi_m\left(\frac{z}{L}\right) \quad \text{et} \quad -\frac{\kappa z u^*}{Q_0}\frac{\partial \bar{\theta}}{\partial z}=\phi_h\left(\frac{z}{L}\right)$$

Wyngaard,
Data from 968 Kansas expt
Businger et al., 1971

From the observations:

stable $\quad \phi_m=1+4{,}8\frac{z}{L}$

$\quad \phi_h=1+7{,}8\frac{z}{L}$

unstable $\quad \phi_m=\left(1-19{,}3\frac{z}{L}\right)^{-1/4}$

$\quad \phi_h=\left(1-12\frac{z}{L}\right)^{-1/2}$

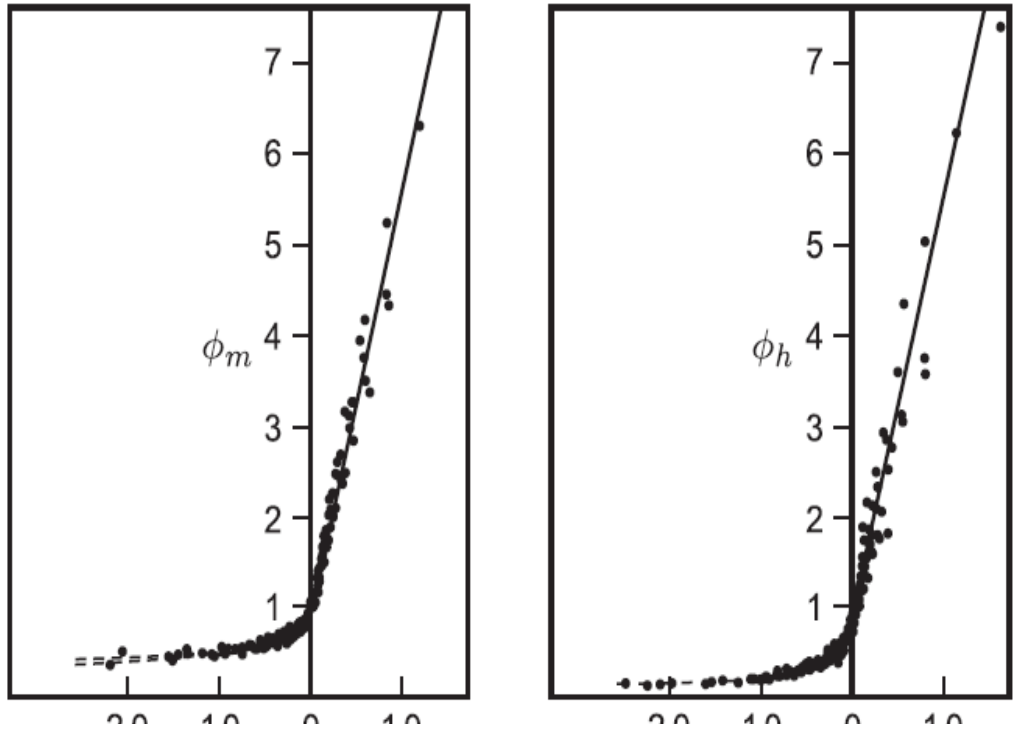

Couche de surface turbulente
Profil de vent en situation convective

stable

$\overline{w'\theta'_v} < 0$

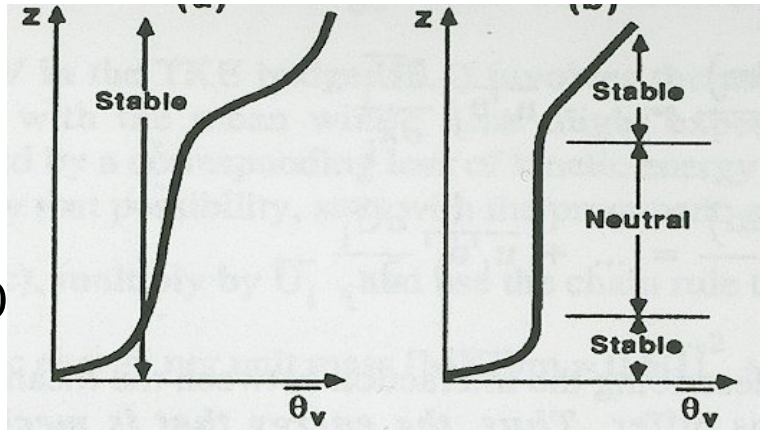

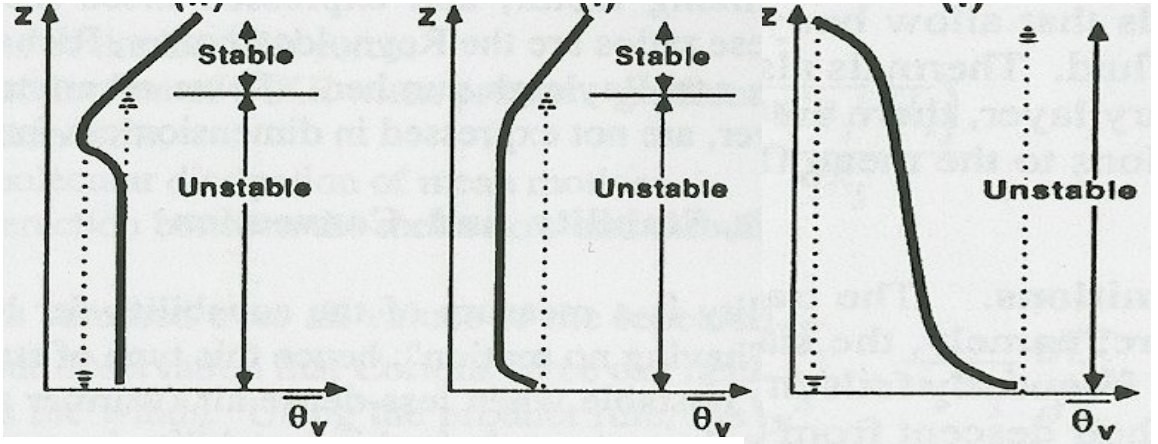

unstable $\overline{w'\theta'_v} > 0$

All the profiles are function of z/L

For example $\frac{\partial U}{\partial z}\frac{\kappa z}{u_*} = \varphi_m\left(\frac{z}{L}\right)$ with $\varphi_m(0) = 1$

Monin-Obukhov Length

$$L = \frac{-\overline{\theta}_v u_*^3}{g\,\kappa\left(\overline{\theta'_v w'}\right)_S}$$

$-10^5\text{m} \le L \le -100\text{m}$	CL unstable
$-100\text{m} < L < 0$	CL very unstable
$0 < L < 10$	CL very stable
$10\text{m} \le L \le 10^5\text{m}$	CL stable
$\lvert L\rvert > 10^5\text{m}$	CL neutral

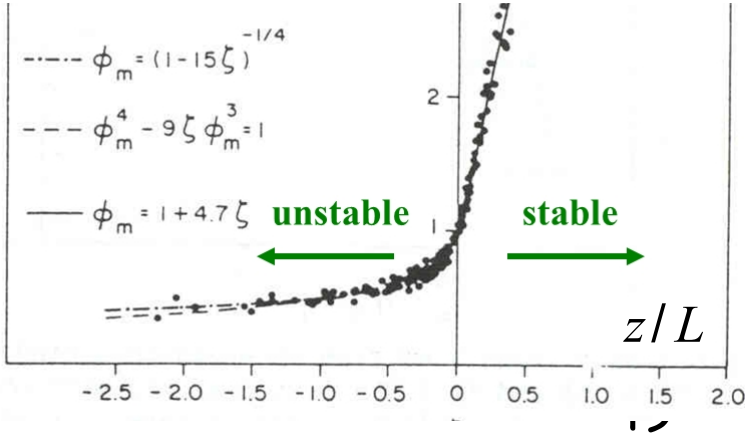

II .10 BACK TO THE MIXING LAYER IN FREE CONVECTION

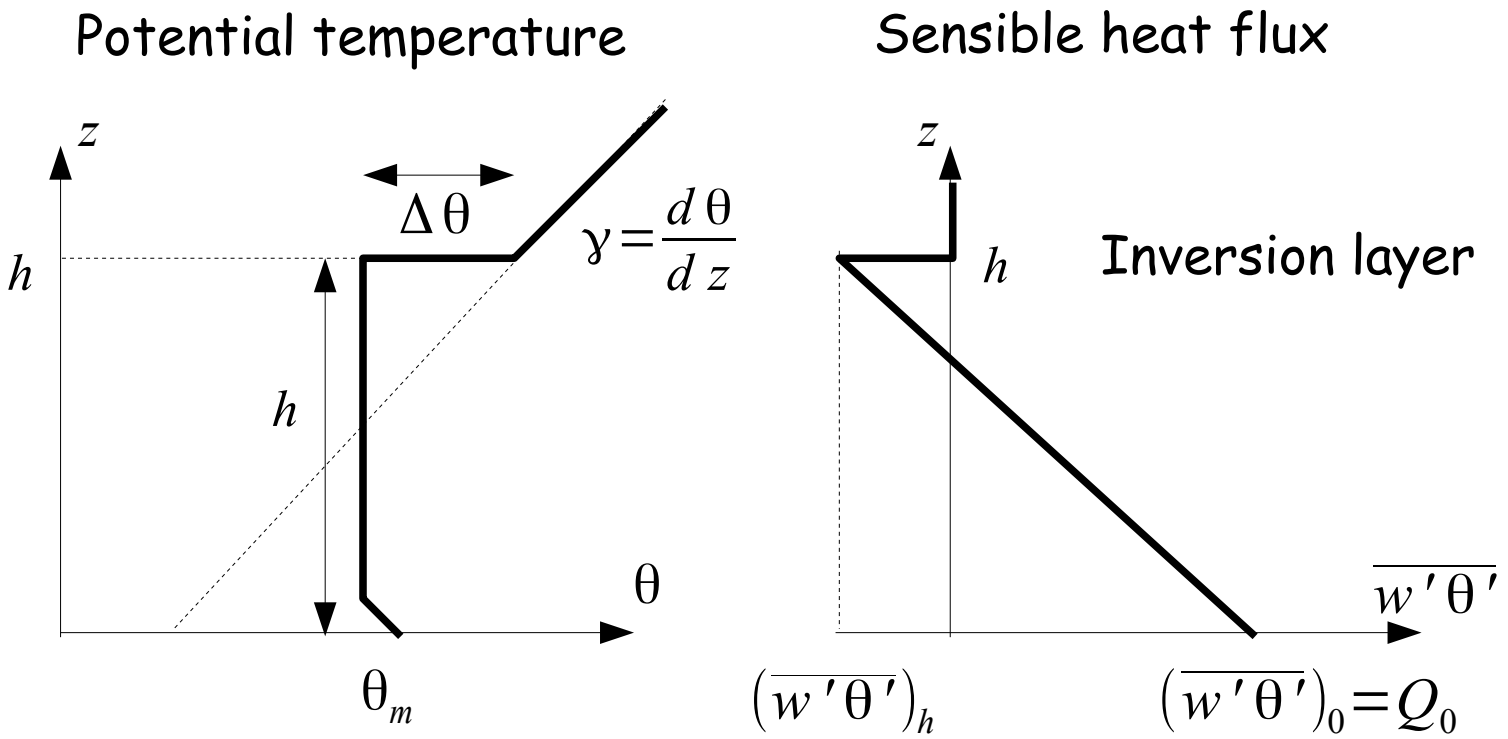

In the mixing layer, the mean gradient vanishes $\frac{\partial \bar{\theta}}{\partial z} = 0$, and $\frac{\partial \bar{\theta}}{\partial t} = -\frac{\partial \overline{w'\theta'}}{\partial z}$

Hence, the flux décreases linearlly with z

Development of an inversion above a boundary layer

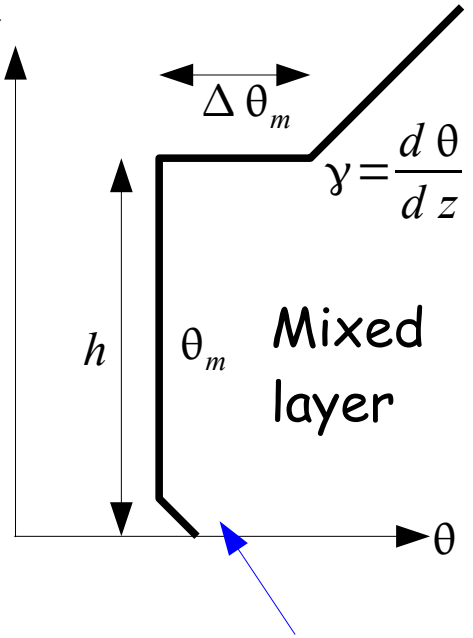

Evolution of θ_m by the difference between top and bottom fluxes:

$$\int_0^h \frac{d\theta}{dt}\,dz = -\int_0^h \frac{\partial}{\partial z}\overline{w'\theta'}\,dz \rightarrow h\frac{d\theta_m}{dt} = (\overline{w'\theta'})_0 - (\overline{w'\theta'})_h$$

Growth of h by entrainment (definition of w_e):

$$\frac{dh}{dt} = w_e$$

Evolution of inversion gap by entrainment and variation of θ_m:

$$\frac{d\Delta\theta_m}{dt} = w_e\gamma - \frac{d\theta_m}{dt}$$

Equilibration between flux and entrainment at the top of the boundary layer:

$$\Delta\theta_m w_e = -(\overline{w'\theta'})_h$$

The solution requires a closure assumption on w_e or $(\overline{w'\theta'})_h$

We choose $(\overline{w'\theta'})_h = -c_E Q_0$ with $Q_0 \equiv (\overline{w'\theta'})_0$ (indpt of t)

Hence $\frac{d\Delta\theta_m}{dt} = \frac{\gamma c_E Q_0}{\Delta\theta_m} - \frac{Q_0(1+c_E)}{h}$ and $\frac{dh}{dt} = \frac{c_E Q_0}{\Delta\theta_m} = w_e$

A solution with $h = \Delta\theta_m = 0$ at $t = 0$ is obtained as $\Delta\theta_m = At^{1/2}$ and $h = Bt^{1/2}$

where $A = \sqrt{\frac{2\gamma c_E^2 Q_0}{1+2c_E}}$ and $B = \sqrt{\frac{2Q_0(1+2c_E)}{\gamma}}$. We get also: $\theta_m = \theta_0 + \sqrt{\frac{2(1+c_E)\gamma Q_0 t}{1+2c_E}}$

The inversion layer which caps convective motion is a direct consequence of the development of a boundary layer

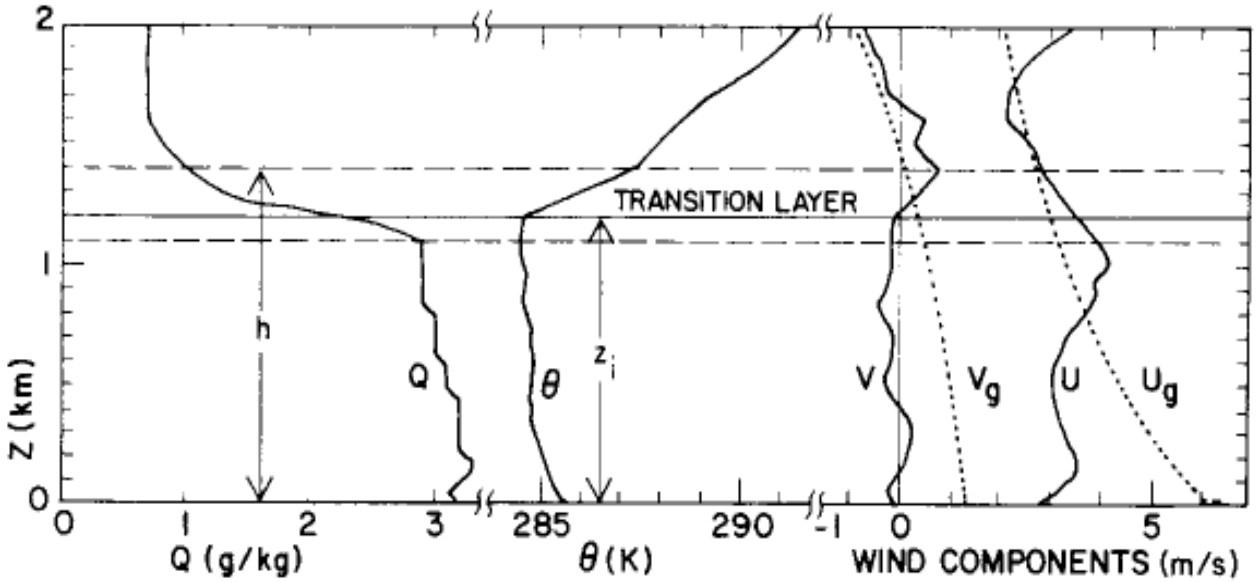

Fig. 6.5 Measured wind, potential temperature, and specific humidity profiles in the PBL under convective conditions on day 33 of the Wangara Experiment. [From Deardorff (1978).]

Typical mixed layer structure of a convective boundary layer (visible even in *u*, *v*).

STABLE BOUNDARY LAYER

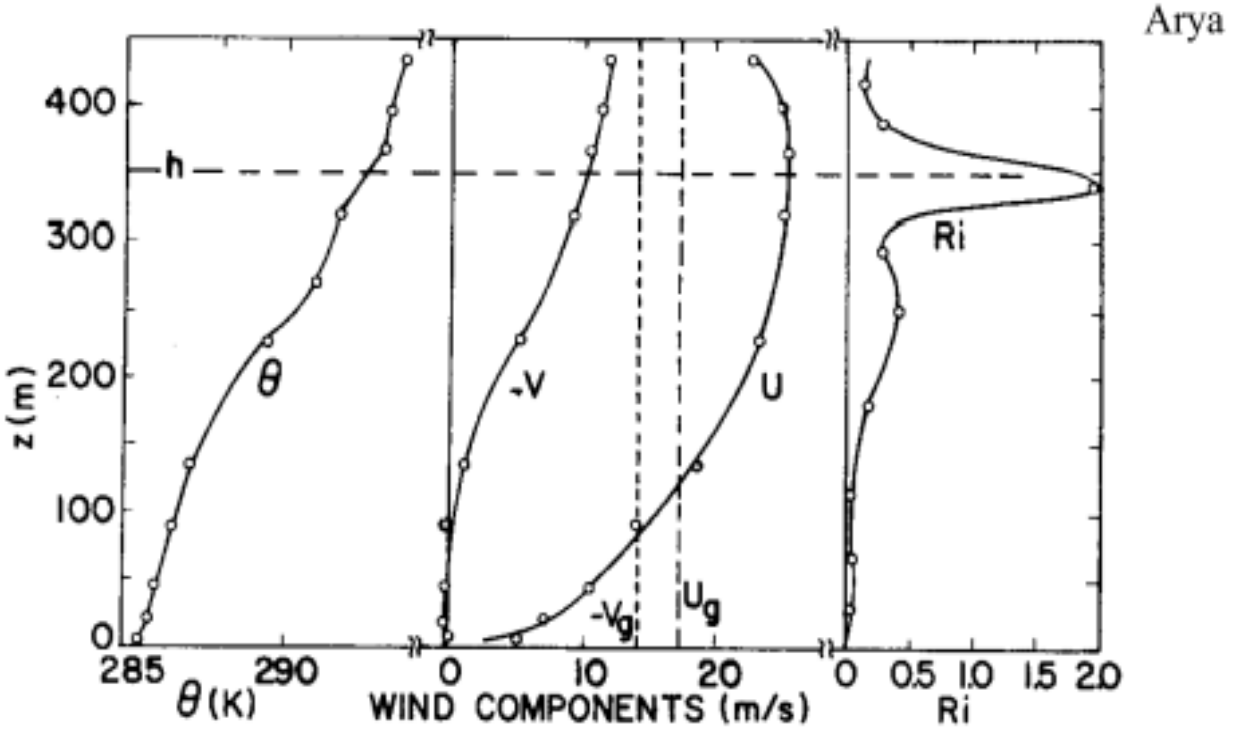

Fig. 6.7 Observed vertical profiles of mean wind components and potential temperature and the calculated Ri profile in the nocturnal PBL under moderately stable conditions. [From Deardorff (1978); after Izumi and Barad (1963).]